ARACINs, Brassicaceae-Specific Peptides Exhibiting Antifungal Activities against Necrotrophic Pathogens in Arabidopsis[1][OPEN]

Jenny Neukermans[2], Annelies Inzé[2], Janick Mathys, Barbara De Coninck, Brigitte van de Cotte, Bruno P.A. Cammue*, and Frank Van Breusegem*

Department of Plant Systems Biology, Vlaams Instituut voor Biotechnologie, B–9052 Ghent, Belgium (J.N., A.I., B.D.C., B.v.d.C., B.P.A.C., F.V.B.); Department of Plant Biotechnology and Bioinformatics, Ghent University, B–9052 Ghent, Belgium (J.N., A.I., B.v.d.C., F.V.B.); and Centre of Microbial and Plant Genetics, Katholieke Universiteit Leuven, 3001 Heverlee, Belgium (J.N., J.M., B.D.C, B.P.A.C.)

Plants have developed a variety of mechanisms to cope with abiotic and biotic stresses. In a previous subcellular localization study of hydrogen peroxide-responsive proteins, two peptides with an unknown function (designated ARACIN1 and ARACIN2) have been identified. These peptides are structurally very similar but are transcriptionally differentially regulated during abiotic stresses during *Botrytis cinerea* infection or after benzothiadiazole and methyl jasmonate treatments. In Arabidopsis (*Arabidopsis thaliana*), these paralogous genes are positioned in tandem within a cluster of pathogen defense-related genes. Both ARACINs are small, cationic, and hydrophobic peptides, known characteristics for antimicrobial peptides. Their genes are expressed in peripheral cell layers prone to pathogen entry and are lineage specific to the Brassicaceae family. In vitro bioassays demonstrated that both ARACIN peptides have a direct antifungal effect against the agronomically and economically important necrotrophic fungi *B. cinerea*, *Alternaria brassicicola*, *Fusarium graminearum*, and *Sclerotinia sclerotiorum* and yeast (*Saccharomyces cerevisiae*). In addition, transgenic Arabidopsis plants that ectopically express *ARACIN1* are protected better against infections with both *B. cinerea* and *A. brassicicola*. Therefore, we can conclude that both ARACINs act as antimicrobial peptides.

During biotic and abiotic stresses, the cellular metabolic status is perturbed, producing a variety of reactive oxygen species (ROS) as a consequence (Van Breusegem et al., 2008; Mittler et al., 2011). In addition to being toxic byproducts of aerobic metabolism, ROS and, more particularly, hydrogen peroxide (H_2O_2) are considered as signaling molecules that trigger signal transduction pathways involved in defense responses and cell death (Apel and Hirt, 2004; Gadjev et al., 2006; Van Breusegem and Dat, 2006). Transcriptome analyses revealed an important enrichment of ROS-responsive genes during biotic and abiotic stresses, including many defense-related genes such as the pathogenesis-related genes (Broekaert et al., 2000; Apel and Hirt, 2004; Torres and Dangl, 2005; Torres et al., 2006; van Loon et al., 2006; Queval et al., 2012). Among them, antimicrobial peptides (AMPs) are considered to play a key role in plant defense, acting both as permanent and inducible defense barriers (García-Olmedo et al., 1998).

Plant AMPs are generally small (12–50 amino acids), cationic, hydrophobic, and secreted peptides that are widespread throughout the plant kingdom and include plant defensins, lipid transfer proteins, hevein- and knottin-type peptides, cyclotides, snakins, maize (*Zea mays*) basic peptide1, and polyprotein precursor AMPs from both *Macadamia integrifolia* and *Impatiens balsamina* (Broekaert et al., 1995; García-Olmedo et al., 1998; Theis and Stahl, 2004; Sels et al., 2008). Due to their amphipathic nature, AMPs are able to permeabilize the pathogen's membrane by both specific and nonspecific electrostatic and hydrophobic interactions with cell surface groups (Shai, 2002; Thevissen et al., 2003; Aerts et al.,

2008). However, increasing evidence shows that the antimicrobial action of some AMPs can be based on more targeted mechanisms, including the interaction with microbe-specific sphingolipids that act as a plant defensin interaction site (Thevissen et al., 2000, 2003, 2004; Wilmes et al., 2011). In addition, AMPs can act as protein translation or enzyme inhibitors, such as α-amylase and protease inhibitors (Broekaert et al., 1997; Lay and Anderson, 2005; Carvalho and Gomes, 2009), or they can inhibit ion channels (Kushmerick et al., 1998; Spelbrink et al., 2004). Interestingly, roles other than antimicrobial activity have been identified (Franco, 2011), i.e. redox regulation (Huang et al., 2008) and development (Takayama et al., 2001; Stotz et al., 2009; Amien et al., 2010).

Overexpression of AMPs has been proposed as a promising strategy to increase disease resistance in transgenic plants (Carvalho and Gomes, 2009, 2011; Visser et al., 2012) thanks to their small size, broad-spectrum activity targeting the pathogen's membrane, and a mode of action that is difficult to develop resistance against (Bulet et al., 2004; Marcos et al., 2008; Eggenberger et al., 2011; Sarika et al., 2012). Overexpression of the radish (*Raphanus sativus*) antifungal peptide RsAFP2 in transgenic *Nicotiana tabacum* plants increased resistance against the fungus *Alternaria longipes* (Terras et al., 1995), while overexpression of an alfalfa (*Medicago sativa*) defensin (*alfAFP*) in transgenic potato (*Solanum tuberosum*) provided high levels of field resistance against *Verticillium dahliae*, the causative agent of the agronomically important early dying disease (Gao et al., 2000). A more advanced and durable approach is to engineer transgenic plants that synthesize chimeras of two or more AMPs with different modes of action to develop a broad-spectrum resistance. For example, overexpression of a chimeric cleavable polyprotein precursor containing the mature domains of the plant defensins *Dahlia merckii* AMP1 (DmAMP1) and RsAFP2 resulted in the efficient release of both bioactive antifungal peptides (François et al., 2002; Thevissen et al., 2004).

AMP overexpression can also confer enhanced tolerance to abiotic stresses (Mirouze et al., 2006; Tamaoki et al., 2008; Lee and Hwang, 2009). For instance, overexpression of the *Capsicum annuum AMP1* (*CaAMP1*) gene in Arabidopsis (*Arabidopsis thaliana*) increased not only resistance against both bacterial and fungal pathogens, but also tolerance to high salt and drought stresses (Lee et al., 2008; Lee and Hwang, 2009). Another example demonstrating the involvement of AMPs in abiotic stress is the zinc stress tolerance in transgenic Arabidopsis lines obtained by overexpression of *PLANT DEFENSIN* (*PDF*) genes of *Arabidopsis halleri* (Mirouze et al., 2006).

Here, we characterized two Arabidopsis AMPs, designated ARACIN1 and ARACIN2, that are transcriptionally regulated by both biotic and abiotic stresses. We demonstrate their antifungal activities in vitro against the broad-host necrotrophic plant fungus *Botrytis cinerea*, the causing agent of gray mold disease, and *Alternaria brassicicola*, which causes black spot disease on members of the Brassicaceae family (Neergaard and Andersen, 1945;

Braverman, 1971; Lawrence et al., 2008). Furthermore, in planta overexpression of *ARACIN1* significantly improved resistance against both pathogens.

RESULTS

Stress and Hormone Responsiveness of *ARACIN1* and *ARACIN2*

Previously, we compiled a comprehensive list of H_2O_2-responsive genes using catalase-deficient Arabidopsis plants exposed to high-light irradiation. Reduced catalase levels, together with high-light exposure, leads to the accumulation of photorespiratory H_2O_2 that, in turn, affects the expression of more than 700 genes (Vanderauwera et al., 2005, 2011; Inzé et al., 2012). ARACIN1 (At5g36925), a peptide of unknown function, was previously identified as nucleocytosolic in a subcellular localization study of H_2O_2-induced proteins (Inzé et al., 2012). The expression of *ARACIN1* and the highly similar paralog *ARACIN2* (At5g36920) was induced (22-fold and 1.35-fold, respectively) by increased levels of photorespiratory H_2O_2.

Due to the absence of representative probe sets on the Affymetrix ATH1 microarray platform, the array-derived expression data on both genes were rather scarce and limited to publicly available data sets that had been obtained from Agilent Arabidopsis V3 arrays and diverse tiling array platforms. From these data sets, we could deduce a down-regulation of *ARACIN1* by abscisic acid and heat stress (Zeller et al., 2009) and an up-regulation in response to *Agrobacterium tumefaciens* infection (Ditt et al., 2006). To complement these array-based abiotic stress-related data, we performed a detailed expression analysis with quantitative PCR on RNA from salt-, cold-, and heat-stressed plants (see "Materials and Methods"). Transcripts of *ARACIN1* were transiently up-regulated by cold stress (5.92-fold after 13 h; Fig. 1A), whereas *ARACIN2* expression remained unaffected. During heat stress, transcripts of *ARACIN1* were substantially down-regulated after 6 and 12 h at 37°C, whereas *ARACIN2* was up-regulated (Fig. 1B).

To investigate the transcriptional regulation of *ARACIN1* and *ARACIN2* during biotic stress, we assessed their transcript levels after infection with the necrotrophic fungus *B. cinerea*. Therefore, 4-week-old Arabidopsis plants were inoculated with *B. cinerea*, and locally and systemically infected leaves were collected 48 h postinoculation. Only *ARACIN2* was strongly induced (16.8-fold) in locally infected leaves, and both genes were induced in systemically infected leaves (Fig. 1C). Further, we assessed their responsiveness toward the defense hormones salicylic acid (SA) and methyl jasmonate (MeJA). Plants were treated with MeJA and benzothiadiazole (BTH), which has an analogous effect to SA and activates the plant's natural defense mechanisms (Lawton et al., 1996; Thomma et al., 2000). After 24 h, the expression of *ARACIN1* was 7-fold higher in
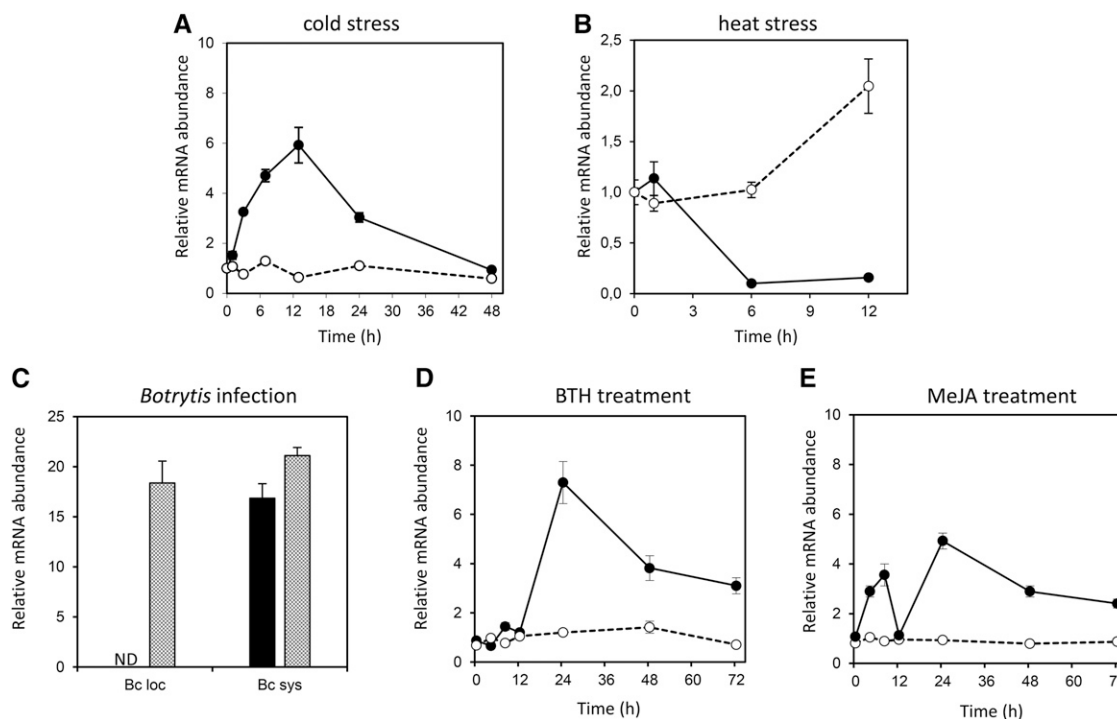
Figure 1. Transcriptional regulation of *ARACIN1* and *ARACIN2*. Relative abundance of *ARACIN1* and *ARACIN2* transcripts after cold stress (A), heat stress (B), *B. cinerea* infection (C), BTH treatment (D), and MeJA treatment (E) represented as fold change relative to wild-type/unstressed or mock-treated values and normalized against ARP7 (A, B, D, and E) or *ELONGATING FACTOR1-α* (*EF1-α*; C; see "Materials and Methods"). Data are the means ± SE (*n* = 3). *ARACIN1* and *ARACIN2* transcript levels are represented by black bars/lines and gray bars/dotted lines, respectively. Bc loc, Local *B. cinerea* infection; Bc sys, systemic *B. cinerea* infection; ND, not detected.

BTH-treated plants than in mock-treated plants and decreased to 3-fold after 72 h (Fig. 1D). By contrast, the expression of *ARACIN2* was not affected by BTH (Fig. 1D). The MeJA response of *ARACIN1* was biphasic: after 4 h, the expression of *ARACIN1* increased almost 3-fold and reached its first maximum after 8 h, returned to basal levels after 12 h, and reached a second maximum after 24 h (Fig. 1E). Again, the expression of *ARACIN2* remained unaffected.

Distinct Spatial Expression of *ARACIN1* and *ARACIN2* Promoters

Expression characteristics were further explored by *GUS* histochemical staining of three independent transgenic plant lines containing constructs in which the *ARACIN1*/*ARACIN2* promoters (intergenic regions; 1,343 and 841 bp, respectively) were transcriptionally fused to *GUS* (Karimi et al., 2007). The expression patterns of *ARACIN1* and *ARACIN2* were spatially distinct (Fig. 2, top). The expression of prom_{ARACIN1}:*GUS* was mainly detected in young developing leaves (Fig. 2A), hydathodes (Fig. 2B), immature flowers (Fig. 2C), and elongating pollen tubes (Fig. 2D), whereas abundant expression levels of prom_{ARACIN2}:*GUS* occurred in young and mature trichomes, hydathodes, the shoot

apical meristem, leaf primordia, the hypocotyl (Fig. 2E), stomatal guard cells (Fig. 2F), and emerging lateral roots (Fig. 2G). In flowers, prom_{ARACIN2}:*GUS* expression was found in the anther-filament junction region and female gametophytes and likely in the embryo sac and the stigma (Fig. 2, H and I). Subsequently, expression analyses, in which both locally infected leaves and noninfected systemic leaves were harvested 3 d post infection (dpi) and incubated with GUS-staining solution, were performed. From this experiment, we could deduce that *ARACIN1* is barely expressed in locally infected leaves around the site of infection, whereas it is highly expressed in systemically infected leaves (Fig. 2, bottom left). *ARACIN2* expression could be shown in both locally and systemically infected leaves (Fig. 2, bottom right). The staining patterns observed are typical for the three independent transgenic plant lines.

ARACIN Genes Are Brassicaceae-Specific Paralogs

ARACIN1 and *ARACIN2* are positioned in tandem on the complement strand of chromosome 5 and are organized as two exons separated by one intron (The Arabidopsis Information Resource [TAIR], http://www.arabidopsis.org/; Fig. 3A). According to the current genome annotation (TAIR10), the open reading
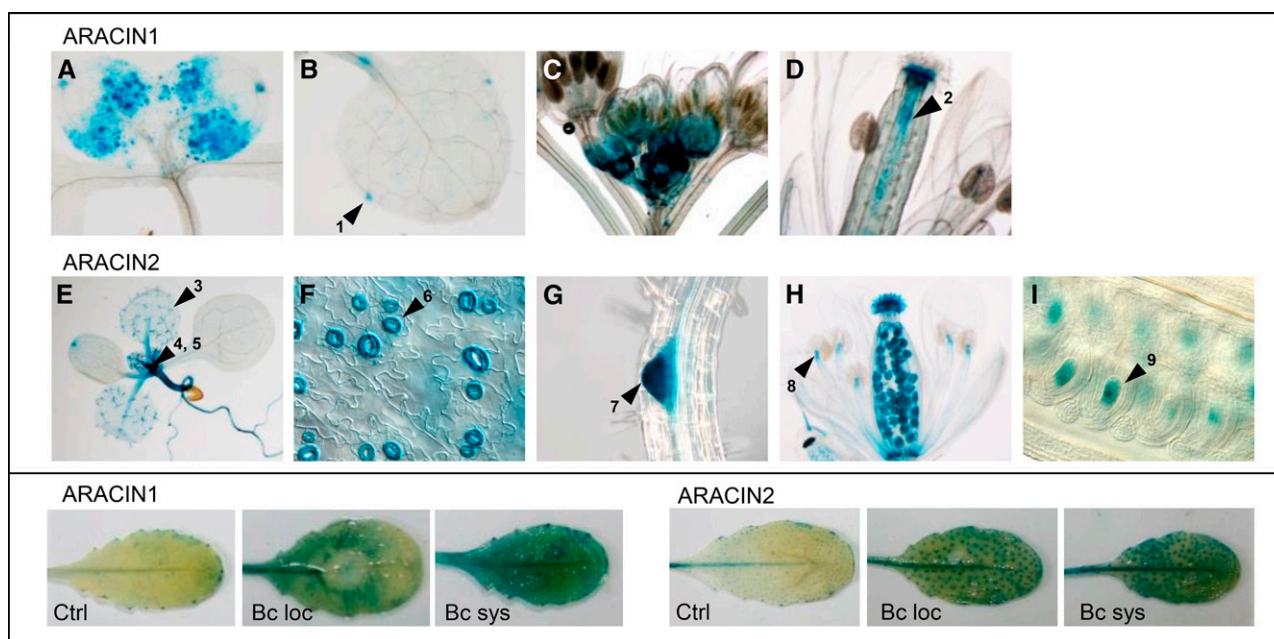
Figure 2. Tissue- and cell-specific expression of *ARACIN1* and *ARACIN2* visualized by histochemical GUS staining without (top) or with (bottom) local infection of *B. cinerea*. A to D, prom$_{ARACIN1}$:*GUS* expression was mainly found in young developing leaves (A), hydathodes indicated by arrow head 1 (B), young developing flowers (C), and in the pollen tube indicated by arrow head 2 (D). E to I, prom$_{ARACIN2}$:*GUS* displayed a strong expression in leaf trichomes (arrow head 3), hydathodes, the shoot apical meristem (arrow head 4), leaf primordia (arrow head 5), the hypocotyl (E), stomata (F, arrow head 6), and emerging lateral roots (G, arrow head 7). In flowers, prom$_{ARACIN2}$:*GUS* expression was found in the junction region between anther and filament (H, arrow head 8) and female gametophytes and likely in the embryo sac (H and I, arrow head 9) and the stigma (H). Bottom left, prom$_{ARACIN1}$:*GUS* expression was mainly detected in systemically infected leaves 3 dpi with *B. cinerea*. Bottom right, prom$_{ARACIN2}$:*GUS* expression could be observed in both locally and systemically infected leaves 3 dpi with *B. cinerea*. Ctrl, No infection; Bc loc, local *B. cinerea* infection; Bc sys, systemic *B. cinerea* infection.

frames (ORFs) of *ARACIN1* and *ARACIN2* are short (192 and 249 nucleotides [nt], respectively) and share 80% coding sequence (CDS) identity (Fig. 3B). However, a misannotation is assumed, because preceding the annotated CDS of *ARACIN1* (designated Δ *ARACIN1*), a sequence was found that was highly similar to the first 54 nt of the CDS of *ARACIN2*, containing a start codon (Fig. 3B) preceded by an adequate Kozak consensus sequence. This was confirmed by 5′ RACE (data not shown), and as such, we can assume that *ARACIN1* and *ARACIN2* encode peptides of 76 (8.2 kD) and 82 amino acids (8.9 kD), respectively (Fig. 3C).

We assessed the presence of *ARACIN1* and *ARACIN2* in other plant genomes by using the PLAZA comparative genomics tool (Proost et al., 2014; http://bioinformatics.psb.ugent.be/plaza/) and blasting National Center for Biotechnology Information (http://www.ncbi.nlm.nih.gov/blast/) and Uniprot databases (http://uniprot.org/blast/), as well as the *Camelina sativa* (http://www.camelinadb.ca/), *Brassica rapa*, and *Brassica oleracea* genomes using the *Brassica* Database (http://brassicadb.org/brad/index.php/). PLAZA 3.0 integrates structural and functional annotations of 31 species. Comparative analysis revealed orthologs of *ARACIN1* and *ARACIN2* in *Arabidopsis lyrata* (Al7g33690 and Al7g33670, respectively), and orthologs for *ARACIN1* could be found

further in *Eutrema salsugineum*, *C. sativa*, *B. rapa*, and *B. oleracea*. For *ARACIN2*, an ortholog could be detected in *Capsella rubella* (Supplemental Fig. S1, A and B).

Analysis of the 5′ sequence upstream of the *ARACIN1* CDS for cis-acting regulatory elements revealed one putative MYC2-binding site (a CACATG sequence located at 849 nt upstream of the *ARACIN1* start codon) that is absent in the *ARACIN2* promoter. MYC2 differentially regulates jasmonic acid-responsive pathogen defense (including *PDF1.2a*) and wound response genes (Lorenzo et al., 2004). Whereas the promoter of *ARACIN1* contains four clustered W-box elements (-255, -227, -208, and -149), the promoter of *ARACIN2* has only two dispersed W-box elements (-718 and -246). These W-box elements are bound with high affinity by WRKY transcription factors known to be involved in SA signaling and plant immunity (Pandey and Somssich, 2009). The presence of multiple MYC2 and W-box elements in the promoter of *ARACIN1* could explain its up-regulation by MeJA and BTH.

ARACIN1 and ARACIN2 Are Targeted to the Endoplasmic Reticulum

Previously, we demonstrated that the N-terminal GFP fusion of Δ ARACIN1, as indicated in TAIR10,
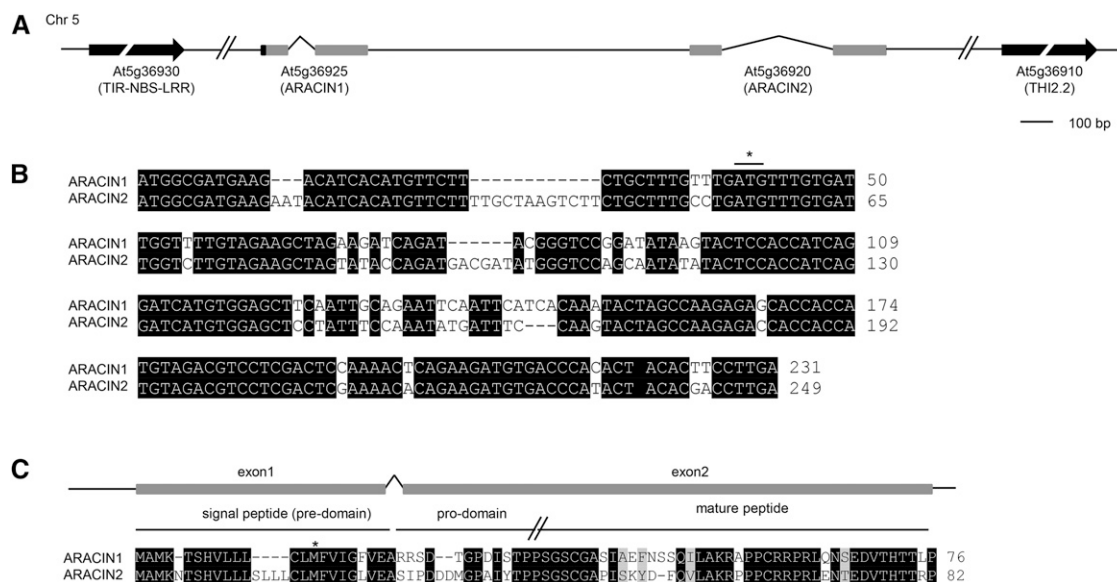
Figure 3. Sequence characteristics of *ARACIN1* and *ARACIN2*. A, Genomic position and gene organization of *ARACIN1* and *ARACIN2*. The 5' region upstream of *ARACIN1* that has a high sequence identity with the 5' CDS of *ARACIN2* is depicted by a black box. B, Sequence alignment of *ARACIN1* and *ARACIN2* revealing a 54-nt sequence upstream of the annotated start codon (asterisk) of *ARACIN1* that is highly similar to the 5' CDS of *ARACIN2*. C, Sequence alignment of the translated full-length ARACIN1 with the protein sequence of ARACIN2. The predicted signal peptide (SignalP 3.0; Emanuelsson et al. ,2007), the first Met according to the TAIR annotation (asterisk), the prodomain, and the highly conserved C-terminal domain (see further) are indicated, as well as the first and second exon. Identical and similar residues are shaded black and gray, respectively. Sequence data were retrieved from TAIR (TAIR10; http://www.arabidopsis.org/). TIR, Toll/Interleukin1 receptor; NBB, nucleotide-binding site; LRR, Leu-rich repeat.

localizes to the nucleus and cytosol (Inzé et al., 2012). Constitutive overexpression of this GFP-tagged nucleosolic version of *ARACIN1* led to a drastic phenotype characterized by a severe loss in apical dominance, resulting in a small bushy stature, thick and contorted leaves, and a delayed flowering time (Supplemental Fig. S2, A–D).

In silico prediction with SignalP3.0 (Emanuelsson et al., 2007) deduced the presence of a signal peptide in ARACIN2 for targeting to the secretory pathway (Fig. 3C), whereas Δ *ARACIN1* was predicted to be cytosolic. However, adding the sequence that was found highly similar to the first 54 nt of the CDS of *ARACIN2* also indicated the presence of an intact N-terminal signal peptide in ARACIN1 for targeting to the secretory pathway (Fig. 3C; Emanuelsson et al., 2007).

To determine the subcellular localization of full-length ARACIN1 and ARACIN2, their ORFs were fused in frame with *GFP* at the C terminus and placed under the control of the constitutive *Cauliflower mosaic virus* 35S (CaMV35S) promoter (Fig. 4A). The subcellular localization of ARACIN1 was assessed in at least two independent and stable transgenic Arabidopsis lines. In the case of *ARACIN2-GFP* overexpression, only one GFP-positive transgenic Arabidopsis line could be obtained. Strikingly, this line showed a similar phenotype as the *GFP-Δ ARACIN1*[OE] (Supplemental Fig. S2, E and F) and *ARACIN2*[OE] lines (see further).

As expected, the addition of the 5' sequence altered the subcellular localization of ARACIN1 (Fig. 4B). Both

localization patterns of ARACIN1-GFP (Fig. 4B, 1 and 2) and ARACIN2-GFP (Fig. 4B, 3 and 4) showed characteristic features of endoplasmic reticulum (ER) localization, such as a reticular pattern and the perinuclear ring (Fig. 4B, 3 and 4), indicating that both ARACIN1 and ARACIN2 are presumably targeted to the ER. This reticular pattern could be further strengthened by coinfiltration in *Nicotiana benthamiana* of ARACIN1-GFP (Fig. 4C, 1–3) or ARACIN2-GFP (Fig. 4C, 4–6) with an ER-mCherry marker created by Nelson et al. (2007).

Interestingly, while expression of the nucleocytosolic-targeted *GFP-Δ ARACIN1* drastically perturbed normal growth and development (Supplemental Fig. S2, A–D), constitutive ER-localized *ARACIN1-GFP* overexpression plants looked phenotypically similar to the wild type (data not shown). Mistargeting of ARACIN1 could perturb the cellular homeostasis, which, in turn, could lead to pleiotropic defects in normal growth and development.

ARACINs Are Typical AMPs

Both ARACINs strikingly share general characteristics of plant AMPs. First, ARACIN1 and ARACIN2 are small (8.2 and 8.9 kD), hydrophobic (39% and 40% total hydrophobic ratios), and cationic (+4 and +2 total net charge) peptides. These features are a prerequisite for the antimicrobial activity of most AMPs that is mainly based on their ability to disturb the pathogen's
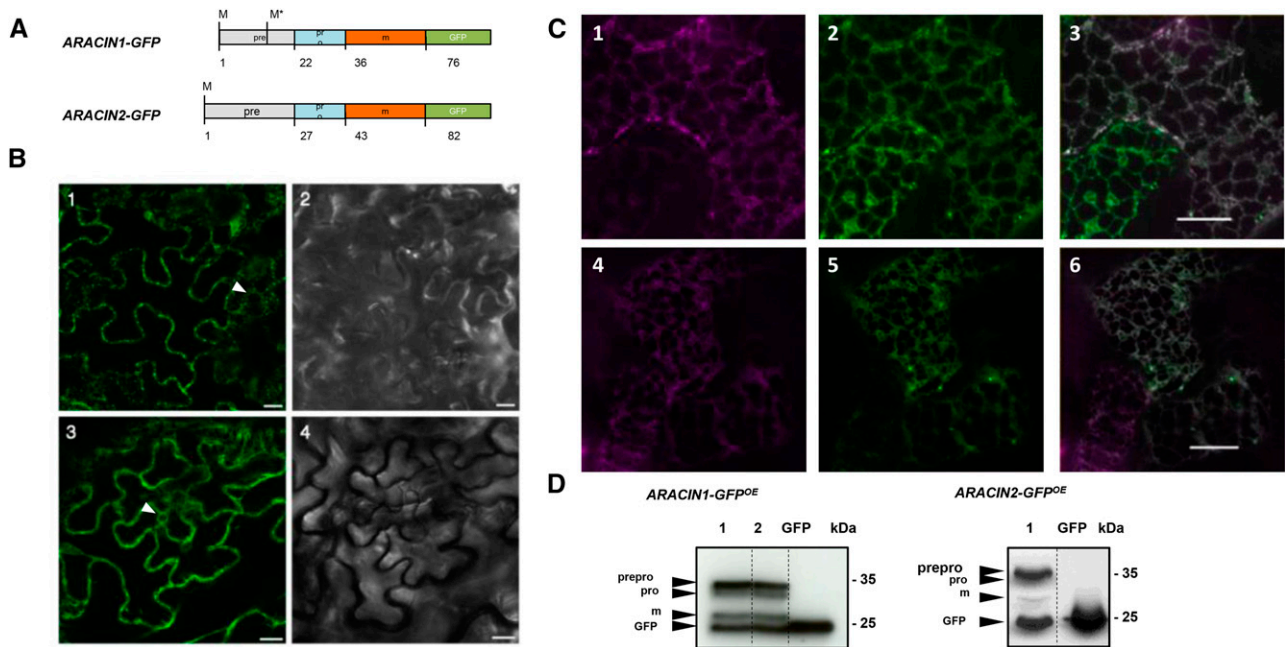
Figure 4. Subcellular targeting and processing of ARACIN1 and ARACIN2. A, Schematic representations of the expressed GFP-tagged peptides with their putative prepropeptide structure used to determine the subcellular localization and processing of ARACIN1 and ARACIN2 in transgenic Arabidopsis lines. The first Met (M) of ARACIN1 according to the TAIR10 annotation (TAIR; http://www.arabidopsis.org/) is indicated with an asterisk. B, Subcellular localizations of the GFP-tagged ARACIN peptides in 2-week-old transgenic Arabidopsis ARACIN1-GFP^OE (1 and 2) and ARACIN2-GFP^OE (3 and 4) lines. GFP fluorescence (1 and 3) and bright-field images (2 and 4) are depicted. Perinuclear ring is indicated with a white arrow head. C, Coexpression of the GFP-tagged ARACIN peptides and ER-mCherry marker in 3-week-old agroinfiltrated *N. benthamiana* leaf epidermal cells. *ARACIN1-GFP* (1–3) or *ARACIN2-GFP* (4–6) lines with an ER-mCherry marker. GFP fluorescence (1 and 4), red fluorescent protein fluorescence (2 and 5), and merged images (3 and 6) are depicted. D, Western-blot analysis of leaf extracts of 2-week-old independent (1 and 2) and stable transgenic *ARACIN1-GFP^OE* (above), *ARACIN2-GFP^OE* (below), and *GFP^OE* lines using an anti-GFP antibody. The different forms (prepropeptide [prepro], propeptide [pro], and mature [m]) are indicated. Bars = 10 μm.

membrane via electrostatic and hydrophobic interactions (Shai, 2002; Thevissen et al., 2003). Like nearly all AMPs, *ARACIN1* and *ARACIN2* have a defined exon/intron structure, with the first exon encoding the signal peptide for targeting to the secretory pathway and the second exon coding for the mature peptide (Silverstein et al., 2005; Fig. 3, A and B).

AMPs are often produced as prepropeptides in which the predomain functions as a signal peptide that is removed during secretion. The prodomain is often acidic and thought to neutralize and, thus, inactivate the basic mature peptide when it is still intracellular. Once secreted, this propeptide is proteolytically removed, thereby activating the mature peptide (García-Olmedo et al., 1998). As the C-terminal regions of both ARACIN peptides were highly conserved (Fig. 3C), they could represent the mature domains necessary for antimicrobial activity. The putative prodomains of ARACIN1 and ARACIN2, which are flanked by their predomain (signal peptide) and mature domain, are acidic (pI 5.96 and 3.42, respectively), and thus these regions could function in the neutralization of the cationic mature domain (pI 8.96 and 9.38, respectively). The biochemical properties of these putatively different forms are given in Supplemental Table S1.

To assess whether ARACINs are processed in vivo, we immunodetected GFP-tagged peptides in two independent transgenic Arabidopsis *ARACIN1-GFP^OE* plants and one *ARACIN2-GFP^OE* plant (Fig. 4D). In the case of ARACIN1-GFP, the anti-GFP antibody recognized four protein bands that correspond in size with the putative preproARACIN1-GFP (approximately 35 kD), the proARACIN1-GFP (approximately 30 kD), the mature ARACIN1-GFP (approximately 31 kD), and free GFP (approximately 27 kD). This was also the case for ARACIN2-GFP. The mature ARACIN1 and ARACIN2 domains had an estimated size of approximately 4 kD, of which the size is similar to that of the conserved C-terminal region (Fig. 4D; Supplemental Table S1).

In Vitro Antifungal Activity against *A. brassicicola* and *B. cinerea*

Next, we assessed the potential antifungal activity of ARACIN1 and ARACIN2 by an in vitro antifungal bioassay. Mature forms of ARACIN1 and ARACIN2 produced by chemical synthesis (Supplemental Table S1) were tested against *A. brassicicola*, *B. cinerea*, *Fusarium graminearum*, *Sclerotinia sclerotiorum*, and yeast (*Saccharomyces*

cerevisiae) by means of a microtiter broth dilution assay (Fig. 5; Supplemental Figure S3). Whereas the mature form of ARACIN1 (mARACIN1) efficiently inhibited the growth of *A. brassicicola* starting at a concentration of 1 μg mL^{-1}, with a 50% growth inhibitory concentration (IC$_{50}$) value of 5.46 μg mL^{-1}, the growth of the *B. cinerea* was almost completely inhibited (95.7%) at a concentration of 10 μg mL^{-1} mARACIN1 with an IC$_{50}$ value of 3.05 μg mL^{-1}. In the case of mARACIN2, the IC$_{50}$ value against *A. brassicicola* was significantly lower (1.55 μg mL^{-1}). Likewise, the antifungal activity of mARACIN2 against *F. graminearum* and yeast (IC$_{50}$ values of 9.06 and 0.76 μg mL^{-1}, respectively) was remarkably increased in comparison with mARACIN1 (IC$_{50}$ values of 28.17 and 6.41 μg mL^{-1}, respectively; Fig. 5). Subsequently, antifungal activity of both ARACIN peptides against *S. sclerotiorum* was similar, with efficient IC$_{50}$ values of 0.73 μg mL^{-1} (mARACIN1) and 0.49 μg mL^{-1} (mARACIN2).

ARACIN1 Overexpression Leads to a Decreased Sensitivity to *A. brassicicola* and *B. cinerea* Infections

To assess the effect of *ARACIN* overexpression on plant development, we made constitutive overexpression lines with the CaMV35S promoter. Northern-blot analysis revealed that several independent transgenic lines contained elevated levels of the *ARACIN1*/*ARACIN2* transcripts (Fig. 6B). Whereas all *ARACIN1*^{OE} lines were phenotypically similar to wild-type plants, overexpression of *ARACIN2* drastically affected growth and development (Fig. 6A). After normal seed germination and cotyledon expansion, *ARACIN2*^{OE} plants showed a severely retarded growth, curled dark leaves, and delayed flowering (Fig. 5B), resembling the observed phenotype of the *ARACIN2-GFP*^{OE} line (Supplemental Fig. S2, E and F).

To assess the effect of increased *ARACIN* levels on the plant susceptibility to fungal infection, we performed disease assays with the two necrotrophic pathogens *A. brassicicola* and *B. cinerea*. Because of the drastic phenotype of the *ARACIN2*^{OE} lines, no accurate scoring of disease symptoms was possible. Therefore, homozygous *ARACIN1*^{OE} plants from three independent transgenic events (Fig. 6B) were assayed with *A. brassicicola* and *B. cinerea* by drop inoculation (5 × 10^5 spores mL^{-1}) of 4-week-old Arabidopsis plants. Compared with the wild type, *ARACIN1*^{OE} lines had an increased resistance phenotype after inoculation with *A. brassicicola*. A drastic reduction of disease symptoms was visible 4 d after infection: the mean lesion size on *ARACIN1*^{OE} leaves was 50% smaller than that on wild-type leaves
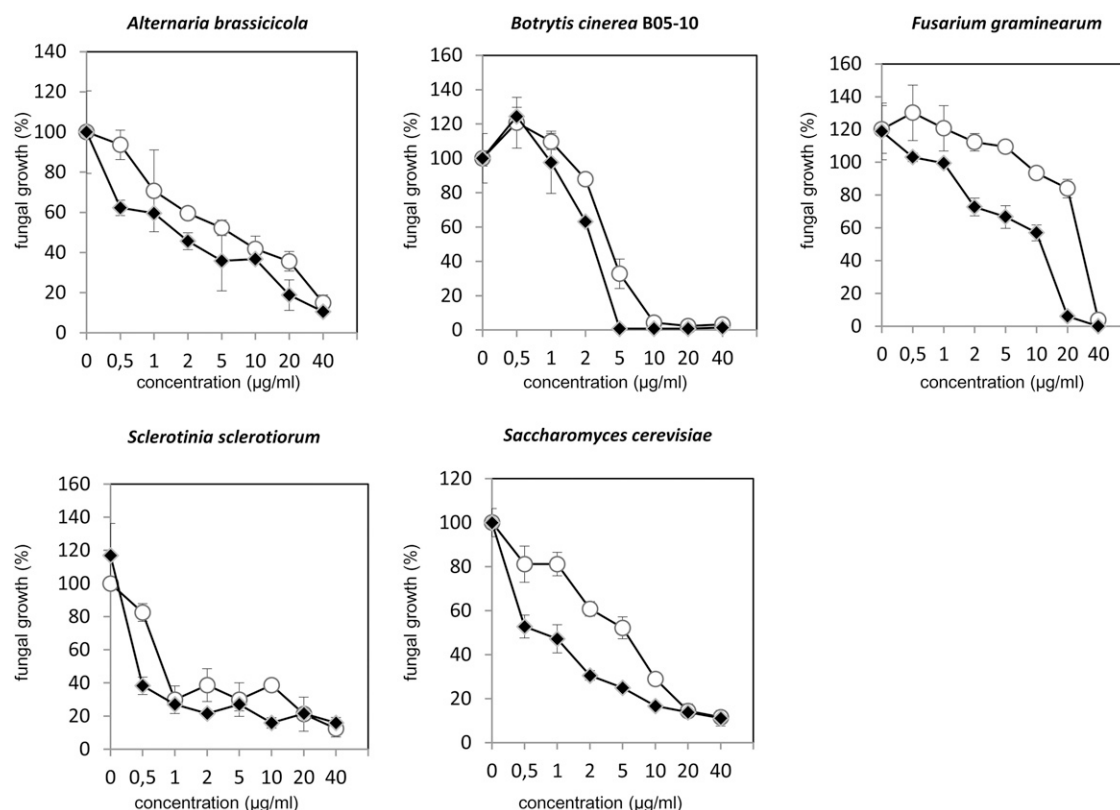
Figure 5. Inhibitory effects of mARACIN1 and mARACIN2 on growth of *A. brassicicola*, *B. cinerea* strain B05-10, *F. graminearum*, *S. sclerotiorum*, and yeast. Data are represented as a mean (*n* = 3). The antifungal assays were done in triplicate, with similar results. ARACIN1 and ARACIN2 are depicted with white and black dots, respectively.
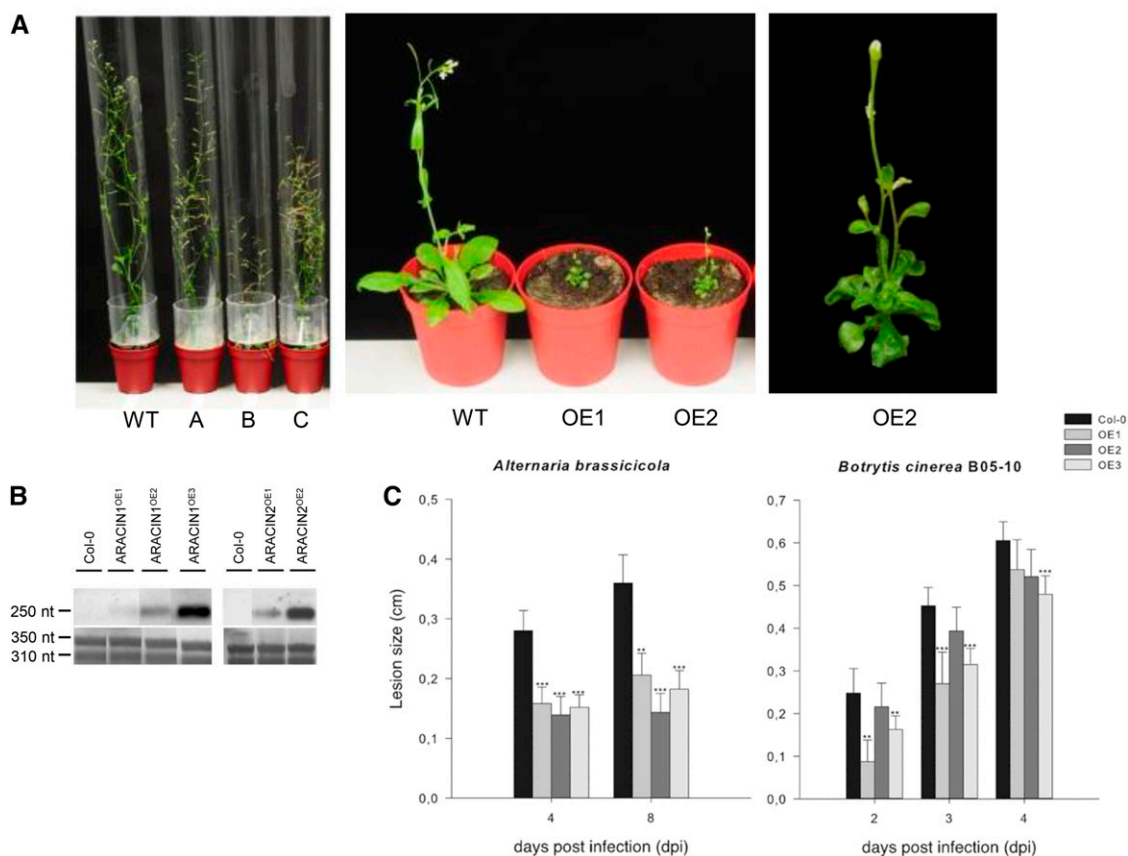
Figure 6. Expression analysis and phenotypes of the *ARACIN*^OE lines. A, Representative images of the *ARACIN1*^OE and *ARACIN2*^OE lines. Left, One 1-month-old wild-type (WT), one *ARACIN1*^OE (A), and two *ARACIN2*^OE (B and C) lines. Middle, One 4-week-old wild-type and two independent *ARACIN2*^OE lines. Right, Enlarged image of a 4-week-old *ARACIN2*^OE plant. B, Northern-blot analysis of the *ARACIN1*^OE and *ARACIN2*^OE lines. Top, *ARACIN1* expression. Bottom, *ACTIN* expression level. C, Lesion sizes on leaves of wild-type plants and three independent *ARACIN1*^OE lines measured several days after inoculation with *A. brassicicola* and *B. cinerea* strain B05-10. Data presented are the means of at least 50 lesions. Error bars represent 95% confidence intervals (*n* = approximately 50). For each assay, the average lesion diameter of wild-type and mutant plants were compared with a Student's *t* test (*$P < 0.05$, **$P < 0.01$, and ***$P < 0.001$). The disease assays were done in duplicate, with similar results. Col-0, Ecotype Columbia; OE, overexpression.

(Fig. 6C). Moreover, a statistically significant reduction in *B. cinerea* lesion size was observed in the *ARACIN1*^OE lines (Fig. 6C).

DISCUSSION

Gene Expression and Genome Organization

Here, we have identified two unique cationic and hydrophobic AMPs. Detailed expression analyses showed that the *ARACIN* genes are differentially regulated by abiotic and biotic stress conditions. It is well known that abiotic stresses, such as high light, high salinity, drought, low and high temperature, or wounding, can also modulate the expression of biotic defense-related genes, including plant AMPs (Hon et al., 1995; Broekaert et al., 2000; Zeier et al., 2004; van Loon et al., 2006; Seo et al., 2008). *ARACIN1* and *ARACIN2* are induced by photorespiratory H_2O_2, a signaling molecule produced

during abiotic and biotic stresses (Fujita et al., 2006). Interestingly, *ARACIN1* is significantly induced by cold stress. The induction of plant AMPs during cold acclimation has been reported previously in winter cereals to confer disease resistance in addition to freezing tolerance (Nakajima and Abe, 1996; Gaudet et al., 1999).

In addition, the cell- and tissue-specific expression patterns of both genes are quite distinct. The differential transcriptional regulation of the *ARACIN* genes could be attributed to their divergent promoters that have a low incidence and small overlap of cis-regulatory elements, and thus these genes are probably under the control of different transcriptional regulators. Duplicated genes (i.e. paralogs) are only retained in the genome when they have acquired different or complementary functions (Tiffin and Moeller, 2006). Therefore, paralogs have often different expression patterns due to changes in the regulatory elements of their promoter region (Force

et al., 1999; Altschmied et al., 2002; Prince and Pickett, 2002).

Recently, 1,789 Brassicaceae-specific genes (including the ARACIN genes) have been identified by a stepwise BLAST filtering approach and are characterized by their short peptide length (77 amino acids), few introns, low guanine-cytosine content, unknown function, few paralogs, enrichment for secretory peptides, and increased evolutionary rates. Remarkably, these Brassicaceae-specific genes are enriched for defensin-like genes and other Cys-rich peptides, such as thionins. These defensin-like genes show higher frequencies of tandem duplications, the major mechanism for the generation of lineage-specific genes. Furthermore, these genes are often responsive to biotic and abiotic stimuli (Donoghue et al., 2011).

Within the Arabidopsis genome, both genes are positioned in tandem and are flanked by pathogen defense-related genes. The gene encoding a disease resistance protein belonging to the Toll/Interleukin1 receptor-nucleotide-binding site-Leu-rich repeat class is positioned upstream of ARACIN1, and a thionin gene (THIONIN2.2) is positioned downstream of ARACIN2. Nucleotide-binding site-Leu-rich repeat resistance genes are part of a large multigene family that might be involved in the first line detection of pathogens (McHale et al., 2006). Defense-related genes are often positioned in gene clusters, allowing a coordinated expression when plant defense is activated (Eckardt, 2007). Moreover, genes that are up-regulated during biotic stress, including Cys-rich AMPs, did expand largely by tandem duplications (Silverstein et al., 2005; Hanada et al., 2008).

Molecular Properties

ARACIN1 and ARACIN2 encode small, cationic, and hydrophobic peptides and are expressed in peripheral cell layers, such as stomata, hydathodes, and roots tissues, representing the primary entry points for pathogens. In addition, both genes are expressed in reproductive tissues that are known to be enriched in AMPs (Jones-Rhoades et al., 2007; Punwani et al., 2007). As pollen grains are often coated with bacterial and fungal spores, AMPs are suggested to protect the female gametophyte during the fertilization phase (Cordts et al., 2001). In addition, an alternative role for plant AMPs has been demonstrated in Torenia fournieri and Arabidopsis, in which secreted defensin-like, Cys-rich polypeptides act as pollen tube attractants (Okuda et al., 2009; Takeuchi and Higashiyama, 2012). In this respect, it is interesting to note that ARACIN1 and ARACIN2 are expressed in the pollen tube and in the female gametophyte, respectively.

We could further demonstrate that ARACIN1 and ARACIN2 are produced as prepropeptides, which is often the case for AMPs (García-Olmedo et al., 1998). However, the exact cleavage sites and hence the exact nature of the different domains of the ARACIN peptides still need to be determined by amino acid sequencing of the bands observed in the ARACIN1-GFP and ARACIN2-GFP overexpression lines.

Both localization patterns of ARACIN1-GFP and ARACIN2-GFP (Fig. 4B) showed characteristic features of ER localization. However, because both peptides lack ER retention signals, they are presumably targeted to the extracellular space. As the fluorescent properties of GFP are lost in the apoplast due to an acidic pH, we could not directly confirm that the ARACIN-GFP peptides are secreted into the extracellular matrix. To circumvent the problems associated with the detection of GFP-tagged proteins in the apoplastic space, fusions with the yellow fluorescent protein Venus, a pH-insensitive variant of GFP, and with the red fluorescent protein were made and are currently being investigated.

Secondary structure prediction with the Protein/Homology/analogY Recognition Engine (PHYRE) Web server (Bennett-Lovsey et al., 2008; Kelley and Sternberg, 2009), which uses template-based homology modeling to construct structural predictions, revealed the presence of two α-helices at the C terminus of ARACIN1 (Supplemental Fig. S4A) and α and β contents in ARACIN2 (Supplemental Fig. S4C). Moreover, homology-based three-dimensional models of ARACIN1 and ARACIN2 were constructed with PHYRE2.0 (intensive mode; Supplemental Fig. S4, D and E). Although no structural matches with a high confidence level could be detected, most predictions had a fold occurring in proteins with a putative defense role. AMPs are rapidly evolving molecules due to pressure imposed by competition among phytopathogens (Silverstein et al., 2005). In other words, the sequence conservation between AMPs is rather limited and, therefore, may explain why only structural matches were retrieved with a low confidence level. Nevertheless, ARACIN1 showed an approximately 42% similarity (best hit; confidence level of 11%) with the 48-amino acid residue neurotoxin-I of sea anemone (Stichodactyla helianthus; Structural Classification of Proteins code d2sh1a; Protein Data Bank code 2SH1; Fogh et al., 1990; Wilcox et al., 1993) that belongs to the defensin superfamily and acts on neuronal voltage-gated sodium channels of Crustaceae (Supplemental Fig. S4, B and D). ARACIN2 predominantly retrieved matches with protease inhibitors (data not shown). This is not surprising, because several AMPs have been reported to act as protease inhibitors (Kim et al., 2009). Moreover, in response to pathogen attack, plants secrete inhibitory peptides that inactivate the proteinases produced by phytopathogenic microorganisms (Ryan, 1990).

We further assessed the potential of both ARACIN peptides to protect plants against necrotrophic pathogens. Transgenic Arabidopsis plants with constitutive ARACIN1 overexpression displayed enhanced resistance against the necrotrophs A. brassicicola and B. cinerea. Although A. brassicicola is considered an incompatible fungal pathogen of Arabidopsis, the molecular basis behind the restriction of the A. brassicicola infection is of great interest. An incompatible Arabidopsis-A. brassicicola

interaction triggers a strong systemic response, inducing the up-regulation of the defense genes *PATHO-GENESIS RELATED-1* and *PDF1.2a* (Penninckx et al., 1996). The current knowledge of the molecular mechanisms underlying the interaction between *A. brassicicola* and members of the Brassicaceae family remains rather limited. Several studies have identified important players of the incompatible interaction of the Arabidopsis-*Alternaria* spp. pathosystem, including antimicrobial compounds (Thomma et al., 1999; Schenk et al., 2003; Oh et al., 2005; Schuhegger et al., 2006; Nafisi et al., 2007). In addition, in vitro antifungal bioassays with chemically synthesized mARACIN1 and mARACIN2 revealed their antifungal activities against *A. brassicicola*, *B. cinerea* strain B05-10, *F. graminearum*, and *S. sclerotiorum*.

Several examples of *AMP* overexpression conferring enhanced tolerance to abiotic stresses are known (Mirouze et al., 2006; Lee and Hwang, 2009). As *ARACIN1* is transcriptionally regulated by abiotic stresses, we assessed whether the *ARACIN1^{OE}* lines displayed an improved tolerance against salt stress (50 and 100 mM NaCl) and oxidative stress (2 μM methyl viologen). However, no statistical significant differences between *ARACIN1^{OE}* lines and appropriate controls (scored by measuring root growth and leaf area) were found (data not shown).

CONCLUSION

Here, we characterized two unique Brassicaceae-specific peptides displaying antifungal activities against necrotrophic pathogens. Both ARACIN1 and ARACIN2 are typical AMPs but are structurally unrelated to known plant AMPs. In planta modulation of *ARACIN1* expression levels enhanced the resistance against these pathogens. As plant diseases caused by *A. brassicicola* and *B. cinerea* infections result in major crop losses, the use of ARACIN peptides in transgenic Brassicaceae species could be an alternative strategy to improve disease resistance.

MATERIALS AND METHODS

Plant Growth Conditions and Treatments

For in vitro experiments, Arabidopsis (*Arabidopsis thaliana*) ecotype Columbia plants (wild type) were, unless stated otherwise, grown until stage 1.04 (fourth leaf 1 mm in size; Boyes et al., 2001) on one-half-strength Murashige and Skoog medium (Duchefa Biochemie; http://www.duchefa.com/), 1% (w/v) Suc, and 0.7% (w/v) agar, pH 5.7, at 21°C and under a 16-h-light/8-h-dark photoperiod, 150 μmol m^{-2} s^{-1} light intensity, and 50% relative humidity. For the cold stress treatment, 3-week-old plants were transferred to 4°C in a controlled environment chamber (Weiss technik; http://www.weiss-gallenkamp.com/) and a pool of 10 plants was harvested at each time point, whereas for the heat stress experiment, plants were transferred to a thermostat cabinet (Lovibond; http://www.lovibond.com/) at 37°C, and three pools of 35 plants were harvested at each time point. For the BTH treatment, plants were sprayed with 350 μM BTH (BION 50 WG, a gift from Syngenta Agro S.A. Spain) or with water (mock), whereas for the MeJA treatment, plants were sprayed with 100 μM MeJA containing 0.001% (v/v) Triton X-100 or with 0.001% (v/v) Triton X-100 in water (mock). A pool of 32 plants was harvested at each time point for each treatment.

Two independent experiments were carried out for all treatments (independent sets of plants sown and treated on different dates).

5' RACE

Total RNA was extracted from wild-type plants with TRI Reagent (Molecular Research Center; http://www.mrcgene.com/). 5' RACE-ready complementary DNA (cDNA) was made with the supplied Smart II oligo and Powerscript reverse transcriptase (BD SMART RACE cDNA Amplification Kit, BD Biosciences; http://www.bdbiosciences.com/), and the reaction was run with the gene-specific primers (Supplemental Table S1) and the supplied universal primer mix. Nested PCR reaction products were gel purified with the Nucleospin gel extraction kit (Macherey and Nagel; http://www.mn-net.com/) and sequenced after cloning into the pENTR/D-TOPO vector (Invitrogen; http://www.invitrogen.com/).

Production of Transgenic Lines

Full-length ORFs (with and without stop codon) were PCR amplified from first strand cDNA of wild-type plants with the high-fidelity Phusion DNA polymerase (Finnzymes OY; http://www.finnzymes.fi/) with gene-specific primers extended with *att*B sites for subsequent Gateway cloning into pDONR221 (Invitrogen; Supplemental Table S1). *GFP* fusions were constructed within the binary destination vector pK7FWG2 (Karimi et al., 2007), resulting in a C-terminal *GFP* fusion under the control of the CaMV35S promoter. Overexpression clones were generated within the binary destination vector pK7WG2 (Karimi et al., 2007). To obtain promoter-*GUS* fusion constructs, the intergenic regions of *ARACIN1* (1,343 bp) and *ARACIN2* (841 bp) were PCR amplified from genomic DNA with promoter-specific primers extended with *att*B sites for subsequent Gateway cloning (Supplemental Table S1). PCR fragments were cloned into Gateway entry vectors and subcloned into the binary destination vector pKGWFS7 (Karimi et al., 2007). All constructs were transformed into the *Agrobacterium tumefaciens* strain C58C1 harboring the virulence plasmid MP90. Arabidopsis wild-type plants were transformed via *A. tumefaciens* floral dip (Clough and Bent, 1998). Homozygous lines with a single transfer DNA locus were selected via segregation analysis for hygromicine resistance, and transgene expression was monitored via northern analysis and quantitative reverse transcription (qRT)-PCR analysis for the overexpression lines, GFP fluorescence for the *GFP* fusion lines, or GUS staining for the promoter-*GUS* lines.

Fluorescence Microscopy

The localization in *Nicotiana benthamiana* as well as in stable transformed Arabidopsis was analyzed as described previously (Inzé et al., 2012). In addition to the GFP constructs (see above), an ER-targeted mCherry (Nelson et al., 2007) was used.

For fluorescence microscopy, a confocal microscope 100M with software package LSM 510 version 3.2 was used (Zeiss; http://www.zeiss.com/), equipped with a 63× water-corrected objective (numerical aperture, 1.2) to scan the leaf epidermis and underlying cell layers. GFP fluorescence was imaged in a single-channel setting with 488 nm for GFP excitation, whereas mCherry fluorescence was imaged in a single-channel setting with 543 nm for mCherry excitation.

Promoter GUS Analyses

Transgenic 2-week-old seedlings grown in vitro on one-half-strength Murashige and Skoog plates or organs from mature plants grown in soil were harvested and incubated overnight in 90% (v/v) acetone at 4°C. Acetone was removed, and samples were washed with nullisomic-tetrasomic (NT) buffer (100 mM Tris and 50 mM NaCl, pH 7.0). Next, the NT buffer was replaced with a ferricyanide solution (0.2 mM ferricyanide in NT buffer), and samples were incubated in the dark at 37°C for at least 1 h. Afterward, the ferricyanide solution was replaced with the GUS-staining solution containing 0.02 mM 5-bromo-4-chloro-3-indolyl-D-glucuronide in ferricyanide solution. Samples were placed in the dark at 37°C, incubated for 6 h or overnight, and stored in 100% lactic acid. Samples were photographed with a stereomicroscope (Stemi SV11; Zeiss) or with a Nomarski differential interference contrast microscope BX51 (Olympus; http://www.olympus.com/).

qRT-PCR Analyses

For the abiotic stress expression analyses, RNA isolation, cDNA synthesis, and qRT-PCR analyses were carried out as described in Vanderauwera et al. (2007) with gene-specific primers (Supplemental Table S2). For *ARACIN1* and *ARACIN2*, gene-specific primers were designed with the Beacon Designer software (PremierBiosoft; http://www.premierbiosoft.com/; Supplemental Table S2). *ARP7*, encoding an actin-related protein (At3g60830), was used as a reference gene. The primers for this gene were designed with the Universal ProbeLibrary Assay Design center ProbeFinder software (Roche; https://www.roche-applied-science.com/; Supplemental Table S1). For the qRT-PCR analyses on *Botrytis cinerea*-infected leaves, RNA extraction, DNase treatment, cDNA synthesis, and qRT-PCR experiments were done as described by Mirouze et al. (2006), and *EF1-α* was used as a reference gene. Relative transcript abundance of *ARACIN1* and *ARACIN2* was determined using the Roche LightCycler 480 system and the LC480 SYBR Green I Master kit (Roche Diagnostics). Measurements were taken for three biological and three technical repeats. The amplification data were analyzed using the second derivative maximum method, and resulting crossing point values were converted into relative expression values using the comparative cycle threshold method.

Protein Extraction and Western-Blot Analyses

Total protein extracts were prepared by grinding leaf material (100 mg) in 200 μL of extraction buffer (100 mM HEPES [pH 7.5], 1 mM EDTA, 10 mM β-mercaptoethanol, and 1 mM phenylmethanesulfonylfluoride) and a protease inhibitor cocktail (COMPLETE; Roche). Insoluble debris was removed by centrifugation at 20,800g for 15 min at 4°C. Protein concentrations were determined with the Bradford method (Zor and Selinger, 1996). Proteins (10 μg) were separated on a 12.5% SDS-PAGE gel and transferred to a P membrane (Millipore; http://www.millipore.com/). Filters were blocked in 3% (v/v) milk powder in 25 mM Tris-Cl (pH 8), 150 mM NaCl, and 0.05% Tween 20 for at least 1 h at room temperature and incubated overnight at 4°C with anti-GFP (1:5,000) antibody in blocking buffer (JL-8; Clontech Laboratories; http://www.clontech.com/). Antigen-antibody complexes were detected with horseradish peroxidase-conjugated IgG diluted 1:10,000 (Amersham Biosciences) by means of the Western Lightning kit (GE Healthcare; http://gehealthcare.com/). Images were taken using the Biorad Image Lab 3.0 software.

In Vitro Antifungal Activity Assays

Chemically synthesized mARACIN1and mARACIN2 peptides were purchased (greater than 98% purity) from Genscript (http://www.genscript.com/). Stock solutions of 2×10^7 spores mL^{-1} of *Alternaria brassicicola*, *B. cinerea* strain B05-10, and *Fusarium graminearum* were diluted in one-half-strength potato dextrose broth (PDB) to a final concentration of 2×10^4 spores mL^{-1}. In the case of *Sclerotinia sclerotiorum*, fragments from the edges of the mycelium lawns were transferred to 50 mL of one-half-strength PDB and incubated for 24 to 48 h at 21°C with continuous shaking. Aliquots (500 μL) of these cultures were transferred to 2-mL polypropylene microcentrifuge tubes with o-ringed screw caps, each containing five glass beads (1-mm diameter). The mycelium was fragmented by high-speed reciprocal shaking using a Phastprep apparatus (Bio 101/Savant). The obtained mycelium fragment suspensions were 100-fold diluted for use in antifungal activity assays. For yeast (*Saccharomyces cerevisiae*), cell cultures (5×10^4 cells mL^{-1}) were prepared in POTATO DEXTROSE BROTH:YEAST PETONE DEXTROSE medium (95:5) as described previously. After addition of 196-μL aliquots of these spore/cell suspension dilutions or fragmented mycelium to 4 μL of 2-fold dilution series of mARACIN1and mARACIN2 in dimethyl sulfoxide (DMSO; starting from a 100 μg mL^{-1} stock solution) in microtiter plates, the plates were incubated at 23°C for 48 to 72 h or at 30°C for 48 h in the case of yeast. DMSO was used as a negative control. Fungal growth was evaluated both microscopically and by measuring the optical density at 600 nm. Each fungus was tested in duplicate in the microtiter plates, and each assay was repeated twice. For each assay, the average background-corrected optical density at 600 nm of each dilution and the DMSO control were compared with a Student's t test. Dose response curves were calculated to obtain IC$_{50}$ values. To this end, average background-corrected optical densities were converted to percent inhibition, whereas doses were log transformed. Then, either a four-parameter logistic model or a simple linear model was fitted to the data using the drc package in R. The choice of the model was determined by the shape of the dose response curve.

Disease Assays

Mutant and wild-type Arabidopsis plants were grown in soil (DCM Zaai-en stekgrond; De Ceuster Meststoffen N.V.; http://www.dcm.com/) in a growth chamber with at 21°C/18°C day/night temperature and 75% relative humidity under a 12-h-light/12-h-dark photoperiod with a light intensity of approximately 120 μmol m^{-2} s^{-1}. Four-week-old plants were inoculated with *A. brassicicola* strain MUCL20297 (Mycothèque Université Catholique de Louvain) or *B. cinerea* strain B05-10. To this end, a 2×10^7 spores mL^{-1} solution of the pathogen was diluted in one-half-strength (12 g L^{-1}) PDB in water to a final concentration of 5×10^5 spores mL^{-1}. After spotting 5 μL of the diluted spore solution on two leaves per plant, the plants were placed in a humid chamber (100% relative humidity).

For the *B. cinerea* infection expression analyses, eight leaves from noninoculated plants (control) and eight leaves from systemically or locally infected leaves of inoculated plants were collected 48 h post infection. For each treatment, four replicas were harvested and frozen in liquid nitrogen.

For the disease assay, symptoms were scored by measuring and calculating average diameters of the necrotic lesions on various days after pathogen inoculation. This disease assay was repeated twice with an average of 220 plants per assay. For each assay, the average lesion diameter on leaves of wild-type and mutant plants was compared with a Student's t test.

Sequence data from this article can be found in the GenBank/EMBL data libraries under accession numbers 833660 and 833661.

Supplemental Data

The following supplemental materials are available.

Supplemental Figure S1. Presence of ARACIN1 and ARACIN2 in other plant genomes.

Supplemental Figure S2. Several independent GFP-positive transgenic lines that constitutively express *GFP-Δ ARACIN1* or *ARACIN2-GFP* and displayed severe abnormal morphologies.

Supplemental Figure S3. Antifungal activities of mARACIN1 and mARACIN2 against *A. brassicicola*, *B. cinerea* strain B05-10, *F. graminearum*, and *S. sclerotiorum*.

Supplemental Figure S4. Secondary and tertiary structure predictions of ARACIN peptides.

Supplemental Table S1. Peptide characteristics of the putatively different forms of ARACIN1 and ARACIN2.

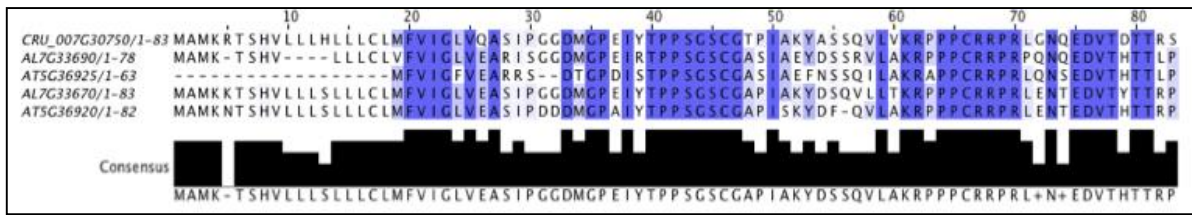**Supplemental Table S2.** PCR primers used in this study.

LITERATURE CITED

Aerts AM, François IE, Cammue BP, Thevissen K (2008) The mode of antifungal action of plant, insect and human defensins. Cell Mol Life Sci **65:** 2069–2079

Altschmied J, Delfgaauw J, Wilde B, Duschl J, Bouneau L, Volff JN, Schartl M (2002) Subfunctionalization of duplicate *mitf* genes associated with differential degeneration of alternative exons in fish. Genetics **161:** 259–267

Amien S, Kliwer I, Márton ML, Debener T, Geiger D, Becker D, Dresselhaus T (2010) Defensin-like ZmES4 mediates pollen tube burst in maize via opening of the potassium channel KZM1. PLoS Biol **8:** e1000388

Apel K, Hirt H (2004) Reactive oxygen species: metabolism, oxidative stress, and signal transduction. Annu Rev Plant Biol **55:** 373–399

Bennett-Lovsey RM, Herbert AD, Sternberg MJ, Kelley LA (2008) Exploring the extremes of sequence/structure space with ensemble fold recognition in the program Phyre. Proteins 70: 611–625

Boyes DC, Zayed AM, Ascenzi R, McCaskill AJ, Hoffman NE, Davis KR, Görlach J (2001) Growth stage-based phenotypic analysis of Arabidopsis: a model for high throughput functional genomics in plants. Plant Cell 13: 1499–1510

Braverman SW (1971) Reaction of broccoli and cauliflower introductions to Alternaria brassicicola. Plant Dis Rep 55: 454–457

Broekaert WF, Cammue BP, DeBolle MF, Thevissen K, DeSamblanx GW, Osborn RW (1997) Antimicrobial peptides from plants. Crit Rev Plant Sci 16: 297–323

Broekaert WF, Terras FR, Cammue BP (2000) Induced and preformed antimicrobial proteins. In AJ Slusarenko, RSS Fraser, LC van Loon, eds, Mechanisms of Resistance to Plant Diseases. Kluwer Academic Publishers, Dordrecht, The Netherlands, pp 371–478

Broekaert WF, Terras FRG, Cammue BP, Osborn RW (1995) Plant defensins: novel antimicrobial peptides as components of the host defense system. Plant Physiol 108: 1353–1358

Bulet P, Stöcklin R, Menin L (2004) Anti-microbial peptides: from invertebrates to vertebrates. Immunol Rev 198: 169–184

Carvalho AO, Gomes VM (2009) Plant defensins: prospects for the biological functions and biotechnological properties. Peptides 30: 1007–1020

Carvalho AO, Gomes VM (2011) Plant defensins and defensin-like peptides: biological activities and biotechnological applications. Curr Pharm Des 17: 4270–4293

Clough SJ, Bent AF (1998) Floral dip: a simplified method for Agrobacterium-mediated transformation of Arabidopsis thaliana. Plant J 16: 735–743

Cordts S, Bantin J, Wittich PE, Kranz E, Lörz H, Dresselhaus T (2001) ZmES genes encode peptides with structural homology to defensins and are specifically expressed in the female gametophyte of maize. Plant J 25: 103–114

Ditt RF, Kerr KF, de Figueiredo P, Delrow J, Comai L, Nester EW (2006) The Arabidopsis thaliana transcriptome in response to Agrobacterium tumefaciens. Mol Plant Microbe Interact 19: 665–681

Donoghue MTA, Keshavaiah C, Swamidatta SH, Spillane C (2011) Evolutionary origins of Brassicaceae specific genes in Arabidopsis thaliana. BMC Evol Biol 11: 47

Eckardt NA (2007) Positive and negative feedback coordinate regulation of disease resistance gene expression. Plant Cell 19: 2700–2702

Eggenberger K, Mink C, Wadhwani P, Ulrich AS, Nick P (2011) Using the peptide BP100 as a cell-penetrating tool for the chemical engineering of actin filaments within living plant cells. ChemBioChem 12: 132–137

Emanuelsson O, Brunak S, von Heijne G, Nielsen H (2007) Locating proteins in the cell using TargetP, SignalP and related tools. Nat Protoc 2: 953–971

Fogh RH, Kem WR, Norton RS (1990) Solution structure of neurotoxin I from the sea anemone Stichodactyla helianthus. A nuclear magnetic resonance, distance geometry, and restrained molecular dynamics study. J Biol Chem 265: 13016–13028

Force A, Lynch M, Pickett FB, Amores A, Yan YL, Postlethwait J (1999) Preservation of duplicate genes by complementary, degenerate mutations. Genetics 151: 1531–1545

Franco OL (2011) Peptide promiscuity: an evolutionary concept for plant defense. FEBS Lett 585: 995–1000

François IE, De Bolle MF, Dwyer G, Goderis IJ, Woutors PF, Verhaert PD, Proost P, Schaaper WM, Cammue BP, Broekaert WF (2002) Transgenic expression in Arabidopsis of a polyprotein construct leading to production of two different antimicrobial proteins. Plant Physiol 128: 1346–1358

Fujita M, Fujita Y, Noutoshi Y, Takahashi F, Narusaka Y, Yamaguchi-Shinozaki K, Shinozaki K (2006) Crosstalk between abiotic and biotic stress responses: a current view from the points of convergence in the stress signaling networks. Curr Opin Plant Biol 9: 436–442

Gadjev I, Vanderauwera S, Gechev TS, Laloi C, Minkov IN, Shulaev V, Apel K, Inzé D, Mittler R, Van Breusegem F (2006) Transcriptomic footprints disclose specificity of reactive oxygen species signaling in Arabidopsis. Plant Physiol 141: 436–445

Gao AG, Hakimi SM, Mittanck CA, Wu Y, Woerner BM, Stark DM, Shah DM, Liang J, Rommens CM (2000) Fungal pathogen protection in potato by expression of a plant defensin peptide. Nat Biotechnol 18: 1307–1310

García-Olmedo F, Molina A, Alamillo JM, Rodríguez-Palenzuéla P (1998) Plant defense peptides. Biopolymers 47: 479–491

Gaudet DA, Laroche A, Yoshida M (1999) Low temperature-wheat-fungal interactions: a carbohydrate connection. Physiol Plant 106: 437–444

Hanada K, Zou C, Lehti-Shiu MD, Shinozaki K, Shiu SH (2008) Importance of lineage-specific expansion of plant tandem duplicates in the adaptive response to environmental stimuli. Plant Physiol 148: 993–1003

Hon WC, Griffith M, Mlynarz A, Kwok YC, Yang DS (1995) Antifreeze proteins in winter rye are similar to pathogenesis-related proteins. Plant Physiol 109: 879–889

Huang GJ, Lai HC, Chang YS, Sheu MJ, Lu TL, Huang SS, Lin YH (2008) Antimicrobial, dehydroascorbate reductase, and monodehydroascorbate reductase activities of defensin from sweet potato [Ipomoea batatas (L.) Lam. 'Tainong 57'] storage roots. J Agric Food Chem 56: 2989–2995

Inzé A, Vanderauwera S, Hoeberichts FA, Vandorpe M, Van Gaever T, Van Breusegem F (2012) A subcellular localization compendium of hydrogen peroxide-induced proteins. Plant Cell Environ 35: 308–320

Jones-Rhoades MW, Borevitz JO, Preuss D (2007) Genome-wide expression profiling of the Arabidopsis female gametophyte identifies families of small, secreted proteins. PLoS Genet 3: 1848–1861

Karimi M, Bleys A, Vanderhaeghen R, Hilson P (2007) Building blocks for plant gene assembly. Plant Physiol 145: 1183–1191

Kelley LA, Sternberg MJ (2009) Protein structure prediction on the Web: a case study using the Phyre server. Nat Protoc 4: 363–371

Kim JY, Park SC, Hwang I, Cheong H, Nah JW, Hahm KS, Park Y (2009) Protease inhibitors from plants with antimicrobial activity. Int J Mol Sci 10: 2860–2872

Kushmerick C, de Souza Castro M, Santos Cruz J, Bloch C Jr, Beirão PS (1998) Functional and structural features of γ-zeathionins, a new class of sodium channel blockers. FEBS Lett 440: 302–306

Lawrence CB, Mitchell TK, Craven KD, Cho Y, Cramer RA Jr, Kim KH (2008) At death's door: Alternaria pathogenicity mechanisms. Plant Pathol J 24: 101–111

Lawton KA, Friedrich L, Hunt M, Weymann K, Delaney T, Kessmann H, Staub T, Ryals J (1996) Benzothiadiazole induces disease resistance in Arabidopsis by activation of the systemic acquired resistance signal transduction pathway. Plant J 10: 71–82

Lay FT, Anderson MA (2005) Defensins: components of the innate immune system in plants. Curr Protein Pept Sci 6: 85–101

Lee SC, Hwang BK (2009) Functional roles of the pepper antimicrobial protein gene, CaAMP1, in abscisic acid signaling, and salt and drought tolerance in Arabidopsis. Planta 229: 383–391

Lee SC, Hwang IS, Choi HW, Hwang BK (2008) Involvement of the pepper antimicrobial protein CaAMP1 gene in broad spectrum disease resistance. Plant Physiol 148: 1004–1020

Lorenzo O, Chico JM, Sánchez-Serrano JJ, Solano R (2004) JASMONATE-INSENSITIVE1 encodes a MYC transcription factor essential to discriminate between different jasmonate-regulated defense responses in Arabidopsis. Plant Cell 16: 1938–1950

Marcos JF, Muñoz A, Pérez-Payá E, Misra S, López-García B (2008) Identification and rational design of novel antimicrobial peptides for plant protection. Annu Rev Phytopathol 46: 273–301

McHale L, Tan X, Koehl P, Michelmore RW (2006) Plant NBS-LRR proteins: adaptable guards. Genome Biol 7: 212

Mirouze M, Sels J, Richard O, Czernic P, Loubet S, Jacquier A, François IE, Cammue BPA, Lebrun M, Berthomieu P, et al (2006) A putative novel role for plant defensins: a defensin from the zinc hyper-accumulating plant, Arabidopsis halleri, confers zinc tolerance. Plant J 47: 329–342

Mittler R, Vanderauwera S, Suzuki N, Miller G, Tognetti VB, Vandepoele K, Gollery M, Shulaev V, Van Breusegem F (2011) ROS signaling: the new wave? Trends Plant Sci 16: 300–309

Nafisi M, Goregaoker S, Botanga CJ, Glawischnig E, Olsen CE, Halkier BA, Glazebrook J (2007) Arabidopsis cytochrome P450 monooxygenase 71A13 catalyzes the conversion of indole-3-acetaldoxime in camalexin synthesis. Plant Cell 19: 2039–2052

Nakajima T, Abe J (1996) Environmental factors affecting expression of resistance to pink snow mold caused by Microdochium nivale in winter wheat. Can J Bot 74: 1783–1788

Neergaard P, Andersen H (1945) Danish species of Alternaria and Stemphylium: taxonomy, parasitism, economical significance. E. Munksgaard, Copenhagen

Nelson BK, Cai X, Nebenführ A (2007) A multicolored set of in vivo organelle markers for co-localization studies in Arabidopsis and other plants. Plant J 51: 1126–1136

Oh IS, Park AR, Bae MS, Kwon SJ, Kim YS, Lee JE, Kang NY, Lee S, Cheong H, Park OK (2005) Secretome analysis reveals an *Arabidopsis* lipase involved in defense against *Alternaria brassicicola*. Plant Cell **17**: 2832–2847

Okuda S, Tsutsui H, Shiina K, Sprunck S, Takeuchi H, Yui R, Kasahara RD, Hamamura Y, Mizukami A, Susaki D, et al (2009) Defensin-like polypeptide LUREs are pollen tube attractants secreted from synergid cells. Nature **458**: 357–361

Pandey SP, Somssich IE (2009) The role of WRKY transcription factors in plant immunity. Plant Physiol **150**: 1648–1655

Penninckx IA, Eggermont K, Terras FRG, Thomma BPHJ, De Samblanx GW, Buchala A, Métraux JP, Manners JM, Broekaert WF (1996) Pathogen-induced systemic activation of a plant defensin gene in *Arabidopsis* follows a salicylic acid-independent pathway. Plant Cell **8**: 2309–2323

Prince VE, Pickett FB (2002) Splitting pairs: the diverging fates of duplicated genes. Nat Rev Genet **3**: 827–837

Proost S, Van Bel M, Vaneechoutte D, Van de Peer Y, Inzé D, Mueller-Roeber B, Vandepoele K (October 16, 2014) PLAZA 3.0: an access point for plant comparative genomics. Nucleic Acids Res http://dx.doi.org/10.1093/nar/gku986

Punwani JA, Rabiger DS, Drews GN (2007) MYB98 positively regulates a battery of synergid-expressed genes encoding filiform apparatus localized proteins. Plant Cell **19**: 2557–2568

Queval G, Neukermans J, Vanderauwera S, Van Breusegem F, Noctor G (2012) Day length is a key regulator of transcriptomic responses to both CO_2 and H_2O_2 in Arabidopsis. Plant Cell Environ **35**: 374–387

Ryan CA (1990) Protease inhibitors in plants: genes for improving defenses against insects and pathogens. Annu Rev Phytopathol **28**: 425–449

Sarika, Iquebal MA, Rai A (2012) Biotic stress resistance in agriculture through antimicrobial peptides. Peptides **36**: 322–330

Schenk PM, Kazan K, Manners JM, Anderson JP, Simpson RS, Wilson IW, Somerville SC, Maclean DJ (2003) Systemic gene expression in Arabidopsis during an incompatible interaction with *Alternaria brassicicola*. Plant Physiol **132**: 999–1010

Schuhegger R, Nafisi M, Mansourova M, Petersen BL, Olsen CE, Svatoš A, Halkier BA, Glawischnig E (2006) CYP71B15 (PAD3) catalyzes the final step in camalexin biosynthesis. Plant Physiol **141**: 1248–1254

Sels J, Mathys J, De Coninck BM, Cammue BP, De Bolle MF (2008) Plant pathogenesis-related (PR) proteins: a focus on PR peptides. Plant Physiol Biochem **46**: 941–950

Seo PJ, Lee AK, Xiang F, Park CM (2008) Molecular and functional profiling of *Arabidopsis pathogenesis-related* genes: insights into their roles in salt response of seed germination. Plant Cell Physiol **49**: 334–344

Shai Y (2002) Mode of action of membrane active antimicrobial peptides. Biopolymers **66**: 236–248

Silverstein KAT, Graham MA, Paape TD, VandenBosch KA (2005) Genome organization of more than 300 defensin-like genes in Arabidopsis. Plant Physiol **138**: 600–610

Spelbrink RG, Dilmac N, Allen A, Smith TJ, Shah DM, Hockerman GH (2004) Differential antifungal and calcium channel-blocking activity among structurally related plant defensins. Plant Physiol **135**: 2055–2067

Stotz HU, Spence B, Wang Y (2009) A defensin from tomato with dual function in defense and development. Plant Mol Biol **71**: 131–143

Takayama S, Shimosato H, Shiba H, Funato M, Che FS, Watanabe M, Iwano M, Isogai A (2001) Direct ligand-receptor complex interaction controls *Brassica* self-incompatibility. Nature **413**: 534–538

Takeuchi H, Higashiyama T (2012) A species-specific cluster of defensin-like genes encodes diffusible pollen tube attractants in Arabidopsis. PLoS Biol **10**: e1001449

Tamaoki M, Freeman JL, Pilon-Smits EAH (2008) Cooperative ethylene and jasmonic acid signaling regulates selenite resistance in Arabidopsis. Plant Physiol **146**: 1219–1230

Terras FR, Eggermont K, Kovaleva V, Raikhel NV, Osborn RW, Kester A, Rees SB, Torrekens S, Van Leuven F, Vanderleyden J, et al (1995) Small cysteine-rich antifungal proteins from radish: their role in host defense. Plant Cell **7**: 573–588

Theis T, Stahl U (2004) Antifungal proteins: targets, mechanisms and prospective applications. Cell Mol Life Sci **61**: 437–455

Thevissen K, Cammue BPA, Lemaire K, Winderickx J, Dickson RC, Lester RL, Ferket KK, Van Even F, Parret AH, Broekaert WF (2000) A gene encoding a sphingolipid biosynthesis enzyme determines the sensitivity of *Saccharomyces cerevisiae* to an antifungal plant defensin from dahlia (*Dahlia merckii*). Proc Natl Acad Sci USA **97**: 9531–9536

Thevissen K, Ferket KK, François IE, Cammue BP (2003) Interactions of antifungal plant defensins with fungal membrane components. Peptides **24**: 1705–1712

Thevissen K, Warnecke DC, François IE, Leipelt M, Heinz E, Ott C, Zähringer U, Thomma BP, Ferket KKA, Cammue BPA (2004) Defensins from insects and plants interact with fungal glucosylceramides. J Biol Chem **279**: 3900–3905

Thomma BP, Eggermont K, Broekaert WF, Cammue BP (2000) Disease development of several fungi on Arabidopsis can be reduced by treatment with methyl jasmonate. Plant Physiol Biochem **38**: 421–427

Thomma BP, Nelissen I, Eggermont K, Broekaert WF (1999) Deficiency in phytoalexin production causes enhanced susceptibility of *Arabidopsis thaliana* to the fungus *Alternaria brassicicola*. Plant J **19**: 163–171

Tiffin P, Moeller DA (2006) Molecular evolution of plant immune system genes. Trends Genet **22**: 662–670

Torres MA, Dangl JL (2005) Functions of the respiratory burst oxidase in biotic interactions, abiotic stress and development. Curr Opin Plant Biol **8**: 397–403

Torres MA, Jones JDG, Dangl JL (2006) Reactive oxygen species signaling in response to pathogens. Plant Physiol **141**: 373–378

Van Breusegem F, Bailey-Serres J, Mittler R (2008) Unraveling the tapestry of networks involving reactive oxygen species in plants. Plant Physiol **147**: 978–984

Van Breusegem F, Dat JF (2006) Reactive oxygen species in plant cell death. Plant Physiol **141**: 384–390

van Loon LC, Rep M, Pieterse CM (2006) Significance of inducible defense-related proteins in infected plants. Annu Rev Phytopathol **44**: 135–162

Vanderauwera S, De Block M, Van de Steene N, van de Cotte B, Metzlaff M, Van Breusegem F (2007) Silencing of poly(ADP-ribose) polymerase in plants alters abiotic stress signal transduction. Proc Natl Acad Sci USA **104**: 15150–15155

Vanderauwera S, Suzuki N, Miller G, van de Cotte B, Morsa S, Ravanat JL, Hegie A, Triantaphylidès C, Shulaev V, Van Montagu MC, et al (2011) Extranuclear protection of chromosomal DNA from oxidative stress. Proc Natl Acad Sci USA **108**: 1711–1716

Vanderauwera S, Zimmermann P, Rombauts S, Vandenabeele S, Langebartels C, Gruissem W, Inzé D, Van Breusegem F (2005) Genome-wide analysis of hydrogen peroxide-regulated gene expression in Arabidopsis reveals a high light-induced transcriptional cluster involved in anthocyanin biosynthesis. Plant Physiol **139**: 806–821

Visser M, Stephan D, Jaynes JM, Burger JT (2012) A transient expression assay for the in planta efficacy screening of an antimicrobial peptide against grapevine bacterial pathogens. Lett Appl Microbiol **54**: 543–551

Wilcox GR, Fogh RH, Norton RS (1993) Refined structure in solution of the sea anemone neurotoxin ShI. J Biol Chem **268**: 24707–24719

Wilmes M, Cammue BP, Sahl HG, Thevissen K (2011) Antibiotic activities of host defense peptides: more to it than lipid bilayer perturbation. Nat Prod Rep **28**: 1350–1358

Zeier J, Pink B, Mueller MJ, Berger S (2004) Light conditions influence specific defence responses in incompatible plant-pathogen interactions: uncoupling systemic resistance from salicylic acid and PR-1 accumulation. Planta **219**: 673–683

Zeller G, Henz SR, Widmer CK, Sachsenberg T, Rätsch G, Weigel D, Laubinger S (2009) Stress-induced changes in the *Arabidopsis thaliana* transcriptome analyzed using whole-genome tiling arrays. Plant J **58**: 1068–1082

Zor T, Selinger Z (1996) Linearization of the Bradford protein assay increases its sensitivity: theoretical and experimental studies. Anal Biochem **236**: 302–308

A   Presence in *Arabidopsis lyrata* and *Capsella rubella*

B   Presence in *Brassica rapa*

Supplemental Figure S1. Presence of *ARACIN1* and *ARACIN2* in other members of the Brassicaceae family.

(A) Multiple protein sequence alignment of ARACIN1 and ARACIN2 with the *A. lyrata* (Al7g33690 and Al7g33670, respectively) and *Capsella rubella* orthologs identified with the PLAZA comparative genomics tool (Proost et al., 2014). Identical and similar residues are shaded dark and light blue, respectively.

(B) Multiple sequence alignments of *ARACIN1* and *ARACIN2* with the *B. rapa* orthologs identified using the Brassica Database (BRAD; http://brassicadb.org/brad/index.php/).
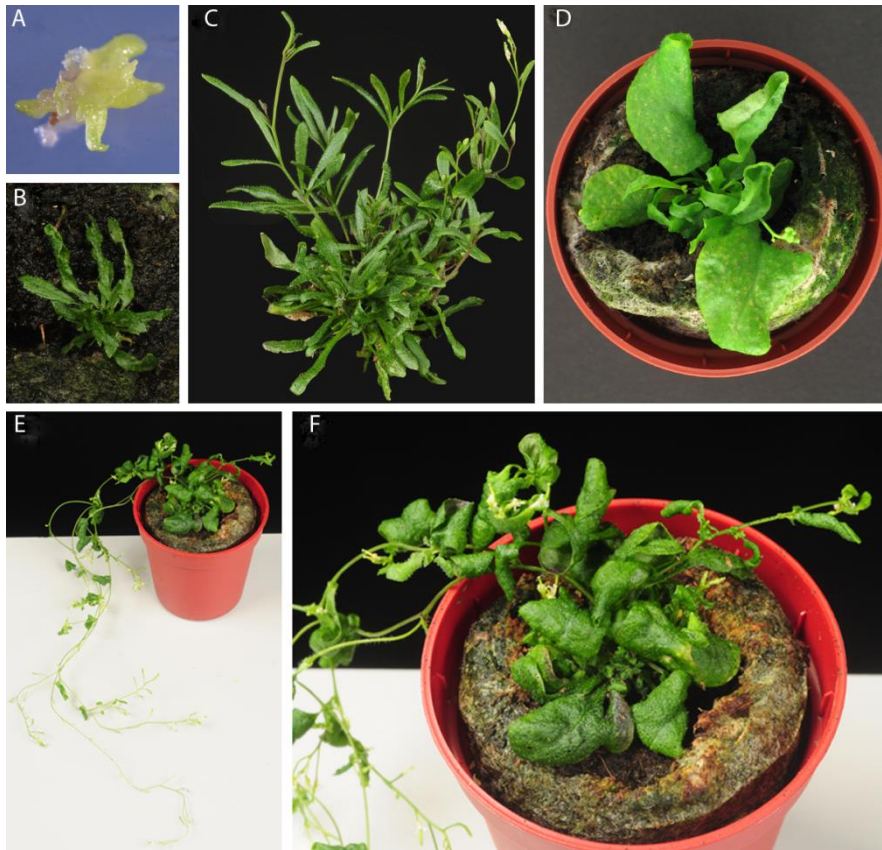
Supplemental Figure S2. Several independent GFP-positive transgenic lines that constitutively express *GFP-Δ ARACIN1* or *ARACIN2-GFP* and displayed severe abnormal morphologies.

(A) Two-week-old primary *GFP-Δ ARACIN1*^{OE} transformant with a callus-like morphology.

(B and C) primary *GFP-Δ ARACIN1*^{OE} transformant (B, 50-day-old; c, 94-day-old) with bushy stature, thick contorted leaves and seedless siliques.

(D) Three-week-old primary *GFP- Δ ARACIN1*^{OE} line displaying a loss in apical dominance and curled leaves.

(E and F) Unique GFP-positive *ARACIN2-GFP*^{OE} plant with severe developmental defects.

Alternaria brassicicola mARACIN1 – 2dpi
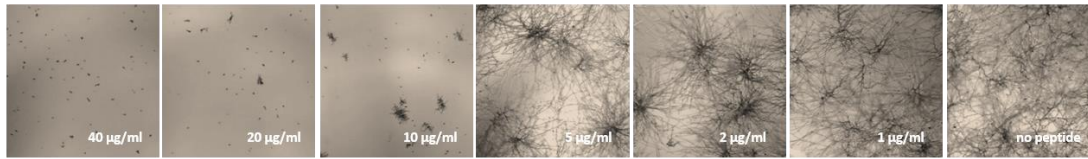
Botrytis cinerae mARACIN1 – 2dpi
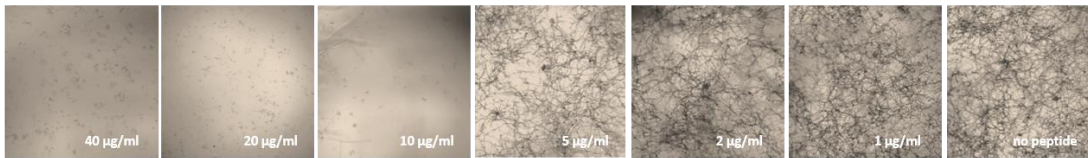
Fusarium graminearum mARACIN1 – 2dpi
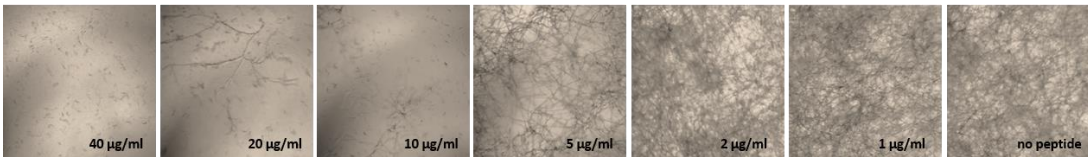
Sclerotinia sclerotiorum mARACIN1 – 3dpi
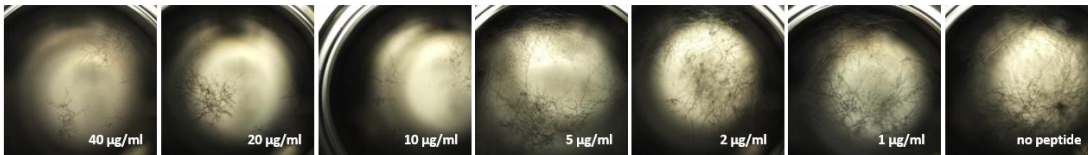
Alternaria brassicicola mARACIN2 – 2dpi
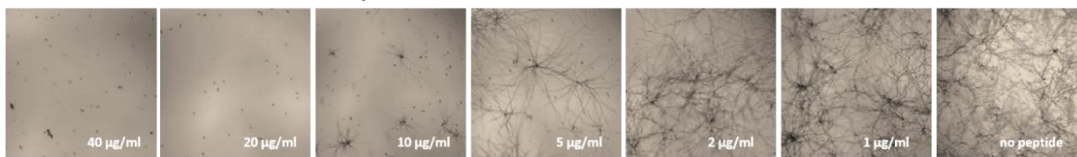
Botrytis cinerae mARACIN2 – 2dpi
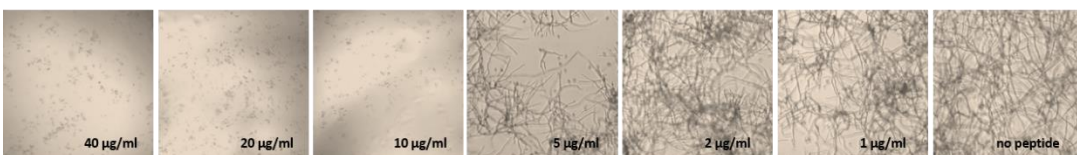
Fusarium graminearum mARACIN2 – 2dpi
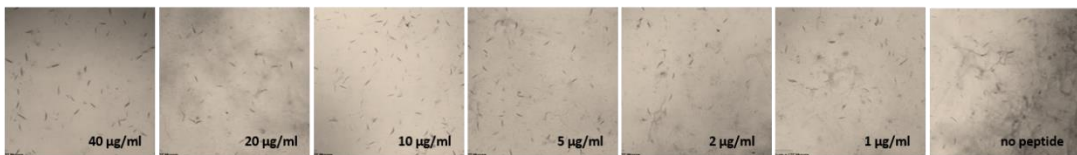
Sclerotinia sclerotiorum mARACIN2 – 3dpi
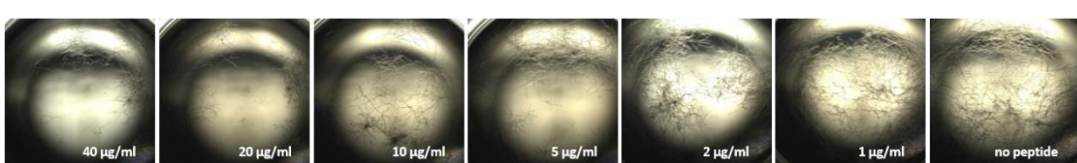
Supplemental Figure S3. Antifungal activities of mARACIN1 and mARACIN2 against *A. brassicicola*, *B. cinerea* B05-10, *F. graminearum* and *S. sclerotiorum*. Pictures were taken 3 dpi.
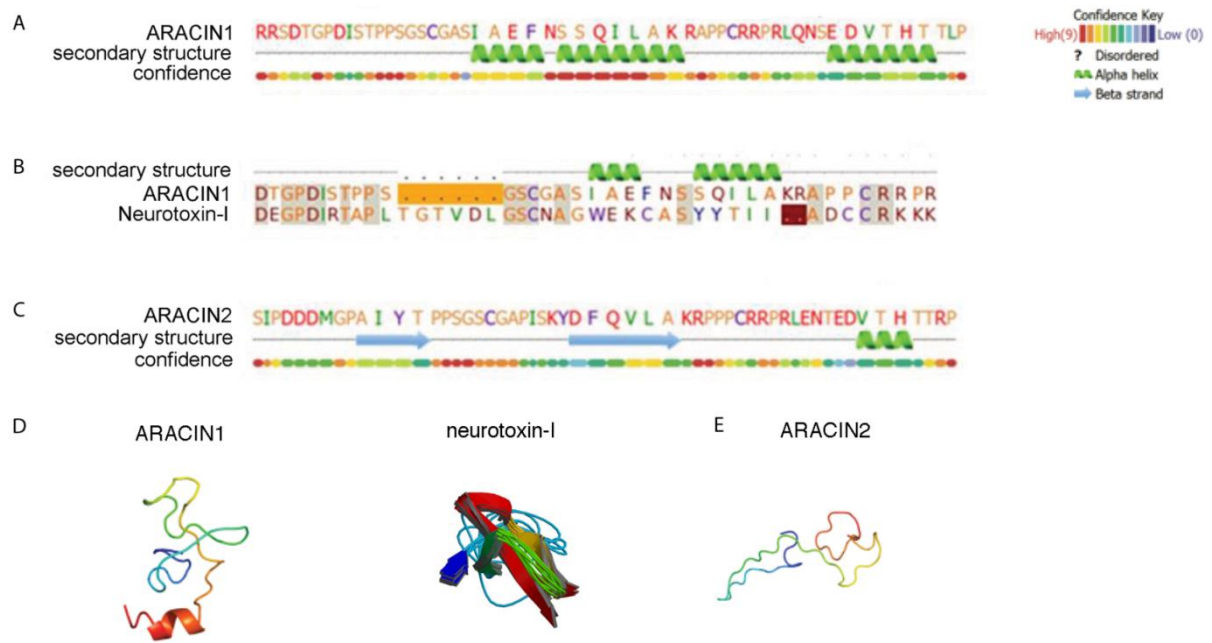
Supplemental Figure S4. Secondary and tertiary structure predictions of ARACIN peptides.
(A) Secondary structure prediction of ARACIN1 by PHYRE (Protein Homology/analogY Recognition Engine; Bennett-Lovsey et al., 2008; Kelley and Sternberg, 2009).
(B) Alignment of ARACIN1 and the 48-amino acid residue neurotoxin-I from *Stichodactyla heliantus* (Fogh et al., 1990; Wilcox et al., 1993).
(C) PHYRE secondary structure prediction of ARACIN2.
(D) Tertiary structure *ab initio* model of ARACIN1 predicted by PHYRE 2.0 (intensive mode). The experimental determined tertiary structure of neurotoxin-I is depicted (Protein Data Bank (PDB) code 2SH1; Fogh et al., 1990; Wilcox et al., 1993).
(E) Tertiary structure *ab initio* model of ARACIN2. Image colored by rainbow N → C terminus.

Supplemental Table 1. Peptide characteristics of the putatively different forms of ARACIN1 and ARACIN2.

The total hydrophobic ratio, total net charge and isoelectric point (pI) of the putative different forms of ARACIN1 and ARACIN2 were calculated with the peptide predictor tool of the Antimicrobial Peptide Database (ADP; http://aps.unmc.edu/AP/main.php/; Wang and Wang (2004)). The sequence length and molecular weight are indicated in number of amino acids (AA) and in kDa, respectively. The predicted signal peptide (SignalP 3.0; Emanuelsson et al. (2007)) is underlined and the sequence of the putative mature peptide is indicated in bold. kDa, kilodalton.

Name	Sequence	Length (AA)	Molecular weight (kDa)	Hydrophobic ratio	Net charge	pI
preproARACIN1	<u>MAMKTSHVLLLCLMFVIGFVE ARRSDTGPDISTPPS</u>**GSCGASI AEFNSSQILAKRAPPCRRPRL QNSEDVTHTTLP**	76	8.2	39%	+4	8.66
proARACIN1	RRSDTGPDISTPPS**GSCGASIAE FNSSQILAKRAPPCRRPRLQN SEDVTHTTLP**	54	5.7	25%	+3	8.95
mARACIN1	**GSCGASIAEFNSSQILAKRAP PCRRPRLQNSEDVTHTTLP**	40	4.2	32%	+3	8.96
preproARACIN2	<u>MAMKNTSHVLLLSLLLCLMFV IGLVEA</u>SIPDDDMGPAIYTPPS **GSCGAPISKYDFQVLAKRPPP CRRPRLENTEDVTHTTRP**	82	8.9	40%	+2	6.70
proARACIN2	SIPDDDMGPAIYTPPS**GSCGAP ISKYDFQVLAKRPPPCRRPRL ENTEDVTHTTRP**	55	5.9	25%	+1	6.49
mARACIN2	**GSCGAPISKYDFQVLAKRPPP CRRPRLENTEDVTHTTRP**	39	4.3	25%	+4	9.38

Wang Z, Wang G (2004) APD: the Antimicrobial Peptide Database. Nucleic Acids Res **32:** D590-D592

Supplemental Table S2. PCR primers used.

Primer name	Gene	Sequence	
At5g36925-TAIR-FW	*ARACIN1*	GGGGACAAGTTTGTACAAAAAAGCAGGCTCCATGTTTGTGATTGGTTTTGTAGAAGCTAG	cloning / genotyping
At5g36925-RV	*ARACIN1*	GGGGACCACTTTGTACAAGAAAGCTGGGTCTCAAGGAAGTGTAGTGTGGGTCAC	cloning / genotyping
At5g36925-no stop-RV	*ARACIN1*	GGGGACCACTTTGTACAAGAAAGCTGGGTCAGGAAGTGTAGTGTGGGTCACATCTTC	cloning / genotyping
PAt5g36925-FW	*ARACIN1*	GGGGACAAGTTTGTACAAAAAAGCAGGCTTCTAACTTATTTGCAGGGAAC	cloning / genotyping
PAt5g36925-RV	*ARACIN1*	GGGGACCACTTTGTACAAGAAAGCTGGGTCCAAACAAAGCAGAAGAAC	cloning / genotyping
PAt5g36925-SIM-RV	*ARACIN1*	GGGGACCACTTTGTACAAGAAAGCTGGGTCTGGCTCTTCTTATCTCAAG	cloning / genotyping
PAt5g36920-FW	*ARACIN2*	GGGGACAAGTTTGTACAAAAAAGCAGGCTTCAAACTAGAAATGTTTCAAGAAG	cloning / genotyping
PAt5g36920-RV	*ARACIN2*	GGGGACCACTTTGTACAAGAAAGCTGGGTCTGGCTCTTCTATCTTAAATAAC	cloning / genotyping
At5g36925-5UTR-FW	*ARACIN1*	GGGGACAAGTTTGTACAAAAAAGCAGGCTTCATGGCGATGAAGACATCAC	cloning / genotyping
At5g36920-FW	*ARACIN2*	GGGGACAAGTTTGTACAAAAAAGCAGGCTTCATGGCGATGAAGAATACATCAC	cloning / genotyping
At5g36920-RV	*ARACIN2*	GGGGACCACTTTGTACAAGAAAGCTGGGTCTCAAGGTCGTGTAGTATGGGTC	cloning / genotyping
At5g36920-NS-RV	*ARACIN2*	GGGGACCACTTTGTACAAGAAAGCTGGGTCAGGTCGTGTAGTATGGGTCAC	cloning / genotyping
At5g36925-FW-SyBr	*ARACIN1*	GTAGAAGCTAGAAGATCAGATAC	qRT-PCR
At5g36925-RV-SyBr	*ARACIN1*	TCAAGGAAGTGTAGTGTGG	qRT-PCR
At5g36920 -FW -SyBr	*ARACIN2*	CTAAGTCTTCTGCTTTGCCTGATG	qRT-PCR
At5g33920 - RV - SyBr	*ARACIN2*	CGTCTACATGGTGGTGGTCTC	qRT-PCR
PR-1_At2g14610-PL-FW	*PATHOGENESIS-RELATED GENE 1*	TGATCCTCGTGGGAATTATGT	qRT-PCR
PR-1_At2g14610-PL-RV	*PATHOGENESIS-RELATED GENE 1*	TGCATGATCACATCATTACTTCAT	qRT-PCR
PR-5_At1g75040-PL-FW	*PATHOGENESIS-RELATED GENE 5*	GACTGTGGCGGTCTAAGATGT	qRT-PCR
PR-5_At1g75040-PL-RV	*PATHOGENESIS-RELATED GENE 5*	TGAATTCAGCCAGAGTGACG	qRT-PCR
Thi2-1_At1g72260-PL-FW	*THIONIN 2.1*	CTGGTCATGGCACAAGTTCA	qRT-PCR
Thi2-1_At1g72260-PL-RV	*THIONIN 2.1*	GCCATTTCTAGCTTGGTTGG	qRT-PCR
Thi2-2_At5g36910-PL-FW	*THIONIN 2.2*	TGACCACTCTCCAAAACTTTGAC	qRT-PCR
Thi2-2_At5g36910-PL-RV	*THIONIN 2.2*	CTTTTAACTGCGGCGGTAGA	qRT-PCR
Pdf1-2_At5g44420-PL-FW	*PLANT DEFENSIN 1.2*	GTTCTCTTTGCTGCTTTCGAC	qRT-PCR
Pdf1-2_At5g44420-PL-RV	*PLANT DEFENSIN 1.2*	GCAAACCCCTGACCATGT	qRT-PCR